ChemInform Abstract: Design, Synthesis and QSAR Studies of Dispiroindole Derivatives as New Antiproliferative Agents.

ARTICLE *in* EUROPEAN JOURNAL OF MEDICINAL CHEMISTRY · AUGUST 2013

Impact Factor: 3.45 · DOI: 10.1016/j.ejmech.2013.07.035 · Source: PubMed

4 AUTHORS:

Riham F George
Cairo University
15 PUBLICATIONS **93** CITATIONS
SEE PROFILE

Nasser S.M. Ismail
Ain Shams University
37 PUBLICATIONS **212** CITATIONS
SEE PROFILE

Jacek Stawiński
Stockholm University
356 PUBLICATIONS **3,478** CITATIONS
SEE PROFILE

Adel S Girgis
National Research Center, Egypt
95 PUBLICATIONS **837** CITATIONS
SEE PROFILE

European Journal of Medicinal Chemistry 68 (2013) 339–351

Contents lists available at ScienceDirect

European Journal of Medicinal Chemistry

journal homepage: http://www.elsevier.com/locate/ejmech

Original article

Design, synthesis and QSAR studies of dispiroindole derivatives as new antiproliferative agents

Riham F. George [a], Nasser S.M. Ismail [b], Jacek Stawinski [c,**], Adel S. Girgis [d,*]

[a] Pharmaceutical Chemistry Department, Faculty of Pharmacy, Cairo University, Cairo, Egypt
[b] Pharmaceutical Chemistry Department, Faculty of Pharmacy, Ain Shams University, Cairo, Egypt
[c] Department of Organic Chemistry, Arrhenius Laboratory, Stockholm University, S-10691 Stockholm, Sweden
[d] Pesticide Chemistry Department, National Research Centre, Dokki, Cairo 12622, Egypt

ARTICLE INFO

Article history:
Received 3 May 2013
Received in revised form
9 July 2013
Accepted 19 July 2013
Available online 11 August 2013

Keywords:
2,6-Bis(arylidene)-1-cyclohexanone
Spiropyrrolidine-oxindole
Azomethine ylide
Antitumor
QSAR

ABSTRACT

A variety of 4′-aryl-3-(arylmethylidene)-1″-[(cyclic-amino)methylene]-1′-methyl-dispiro[cyclohexane-1,3′-pyrrolidine-2′,3″-[3*H*]indole]-2,2″(1″*H*)-diones **4a**–**u** were prepared via reaction of 2*E*,6*E*-bis(arylidene)-1-cyclohexanones **1a**–**i** with azomethine ylides, generated in situ via a decarboxylative condensation of isatins **2a**–**c** and sarcosine (**3**). Single crystal X-ray study of **4a**, revealed structural and stereochemical features of these derivatives. While most of the synthesized compounds exhibit mild antitumor properties when tested against various human tumor cell lines (HEPG2 "liver", HELA "cervical" and PC3 "prostate" cancers), three of them, **4d** and **4p** (active against HEPG2), and compound **4g** (active against HELA), demonstrated higher activities, that were close or even higher than that of the reference standard Doxorubicin. QSAR studies revealed good predictive and statistically significant 3 descriptor models (r^2 = 0.903–0.812, $r^2_{adjusted}$ = 0.855–0.672, $r^2_{prediction}$ = 0.773–0.605).

1. Introduction

Cancer represents one of the most serious clinical problems in the world and its incidence is rising in developing as well as in the developed countries. Despite improved imaging and molecular diagnostic techniques, and advances in prevention and chemotherapeutic management, the disease still affects many millions of patients worldwide [1,2]. Apart from surgical treatment and irradiation techniques, chemotherapy still remains an important option for cancer therapy.

Cancer cells are characterized by unlimited replications, self-sufficiency in growth signals, and insensitivity to antigrowth signals, sustained angiogenesis, metastasis, and evasion of apoptosis [3]. Unfortunately, anticancer agents generally act on metabolically active or rapidly proliferating cells, and cannot distinguish efficiently between cancer and normal cells. Due to usually high toxicity and poor tolerance of the current anticancer agents [4], quest for novel agents with high efficiency, low toxicity, and minimum undesirable side effects is the major imperative of the contemporary drug development research [1].

The most promising new class of heterocyclic molecules having many interesting activity profiles and well-tolerated in human subjects [5,6] are tyrosine kinase inhibitors with antiangiogenic properties [7] bearing a 2-oxindole skeleton as in SU-5416 (semaxanib) **I** and SU-11248 (sunitinib) **II** (Fig. 1). A structurally related compound SU9516 **III** was also reported as a potential inhibitor of cyclic-dependent kinases (CDKs) that can induce apoptosis in colon carcinoma cells [8]. Other important synthetic targets that attracted great attention of many investigators in the last two decades are 2-oxindole analogs with spiropyrrolidine-oxindole structural motif [9]. This framework forms a core structure of many alkaloid and natural products exhibiting potent biological properties [10–13]. The simplest spiropyrrolidine-oxindole found in nature, coerulescine **IV**, displays a local anesthetic effect [14,15], while horsfiline **V** [16–21] (isolated from *Horsfieldia superba*) and elacomine **VI** [22] (isolated from *Elaeagnus commutate*) find use as indigenous medicine. Another members of this family, alstonisine **VII**, a natural alkaloid, was firstly isolated from *Alstonia muelleriana* [23,24], and mitraphylline **VIII**, isolated from *Uncaria tomentosa*, possesses potent antitumor properties against human brain cancer cell lines, neuroblastoma SKN-BE (2) and malignant glioma GAMG [25]. More examples are provided by spirotryprostatins A **IX** and B **X** [26,27],

* Corresponding author. Tel.: +20 2 01220447199; fax: +20 2 33370931.
** Corresponding author. Tel.: +46 8 162485; fax: +46 8 15 49 08.
E-mail addresses: js@organ.su.se (J. Stawinski), girgisas10@yahoo.com, girgisas10@hotmail.com (A.S. Girgis).

0223-5234/$ – see front matter © 2013 Elsevier Masson SAS. All rights reserved.
http://dx.doi.org/10.1016/j.ejmech.2013.07.035

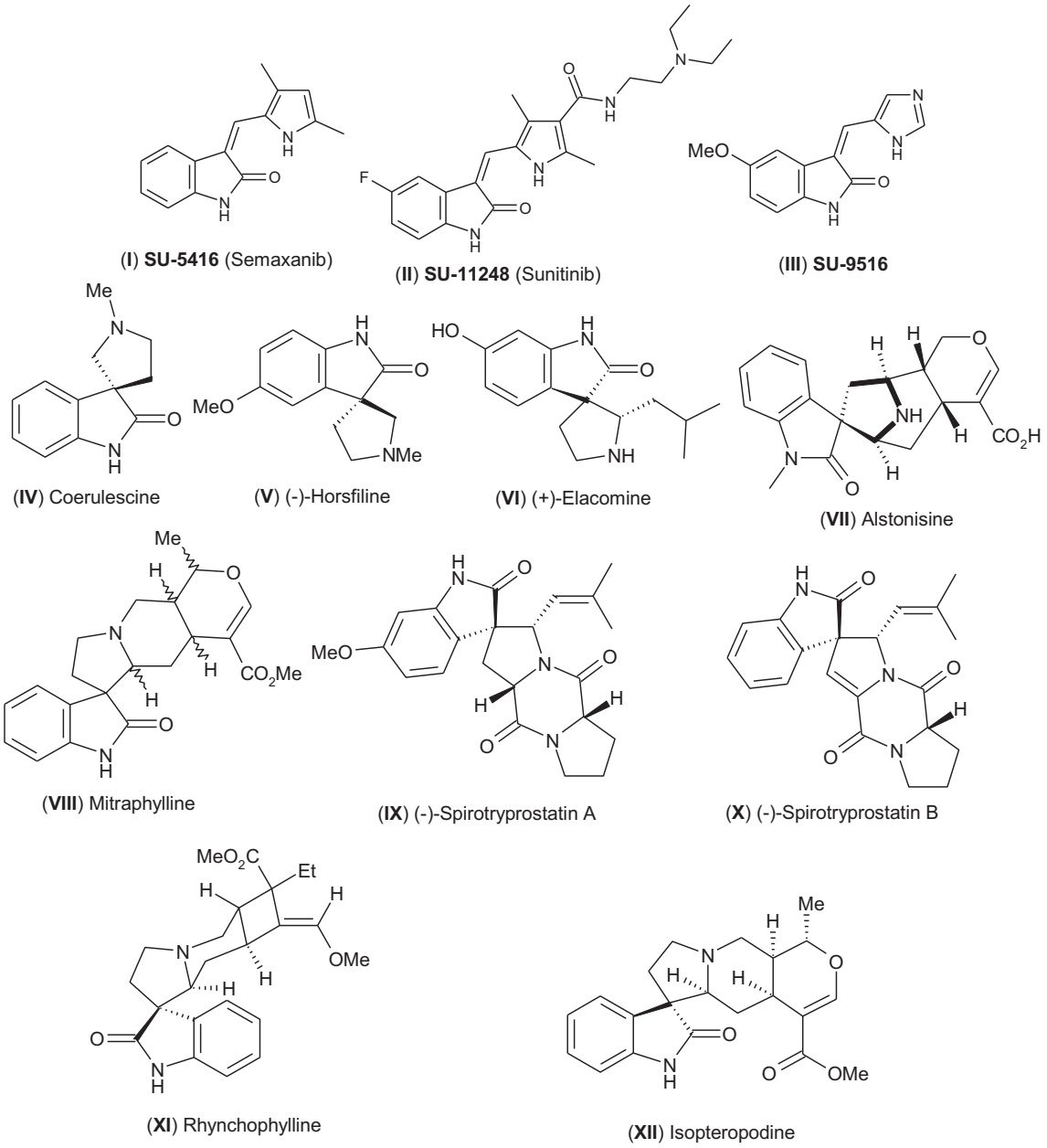

Fig. 1. Pharmacologically active 2-oxindole-containing compounds.

isolated from the fermentation broth of *Aspergillus fumigatus*, that were shown to completely inhibit the G2/M progression of cell division in mammalian tsFT210 cells. Finally, rhynchophylline **XI**, isolated from *Uncaria rhynchophylla*, was found to be antipyretic, anti-hypertensive and anticonvulsant medicine for treatment of epilepsy [28] and a noncompetitive antagonists of the NMDA receptor [29], while isopteropodine **XII**, can efficiently modulate the function of muscarinic and serotonin receptors [30] (Fig. 1).

In the present paper we report on investigations of novel dispiro [cyclohexane-1,3′-pyrrolidine-2′,3″-[3*H*]indole] bearing [(cyclic-amino)methylene] function attached to the indolyl *N*-1″. A possible role of the [(cyclic-amino)methylene] function attached to this position is to provide a positive ionizable residue that may fit our candidate analog in the pharmacophoric active site. Interest in construction of such analogs stems from our previous program directed towards investigation of bio-active agents [31] and the fact that these compounds can be viewed as bio-isosters of dispiro[3*H*-indole-3,2′-pyrrolidine-3′,3″-piperidine]-2(1*H*),4″-diones. The latter compounds were previously synthesized by our group and found to be promising antitumor agents against colon (HCT-116), breast (T-47D), leukemia [HL-60 (TB), MOLT-4, RPMI-8226] and prostate (PC-3) human tumor cell lines [32]. Other dispiroindole derivatives, e.g., dispiro[2*H*-indene-2,3′-pyrrolidine-2′,3″-[3*H*]indole]-1,2″ (1″*H*,3*H*)-diones [33], 1′-methyl-4′-(4-methylphenyl)-dispiro[indane-2,3′-pyrrolidine-2′,3″-indoline]-1,2″-dione [34], and spiro[3*H*-indole-3,2′(1′*H*)-pyrrolo[3,4-*c*]pyrrole]-2,3′,5′(1*H*,2′a*H*,4′*H*)-triones [35], were all found to be antiproliferating agents when screened in various tumor cell lines.

New dispiroindole analogs synthesized within this project were screened against diverse human tumor cell lines, including HEPG2 (liver), HELA (cervical) and PC3 (prostate) cancers, and the rationale for it was as follows. Liver cancer is the sixth leading type of cancers

worldwide, and is also one of the four most prevalent malignant diseases in East Asia and sub-Africa [36]. To date, surgical resection is still the most effective treatment option for liver cancer, but is available only to a small fraction of patients, and the rate recurrence is high. Chemotherapy is also used for the liver cancer patients who are not suitable for surgery, or is applied as an adjuvant treatment in addition to surgery. However, severe toxic side effects, low tumor-selectivity, and highly metastatic and chemo-resistant nature of liver cancer greatly hampered the effectiveness of chemotherapy [37]. Hepatocellular carcinoma usually occurs in patients with chronic liver disease. Infection with hepatitis B or C Virus (HBV, HCV) is the leading cause of this type of cancer, with each virus infection increasing the risk of cancer for more than 10-fold [38]. HCV is considered as a national problem in many countries including ours and the elevated number of hepatocellular carcinoma were observed in the last few years.

The other malignant diseases targeted by our new compounds were cervical cancer, the third most common type of cancer in women almost caused by human papillomavirus (HPV) infection [39], and a prostate cancer, that is one of the most frequently diagnosed non-cutaneous solid cancer in men [40]. The specific causes of prostate cancer remain unknown till date. The risk of death due to metastatic prostate cancer is 1/36. Genetics, age, race, diet, and family history, and even lifestyle may all contribute to prostate cancer risk [41]. The treatment options for prostate cancer are surgery, chemotherapy, cryotherapy, hormonal therapy and/or radiation, but all these are only beneficial at the early stages, with no significant effects after metastasis [42,43]. Therefore, there is a high need for treatments that will stop the metastasis and invasion of prostate cancer cells.

In this paper we present our synthetic studies on the preparation of new dispiroindole derivatives and quantitative structure–activity relationship (QSAR) studies for validation of the observed pharmacological properties of the investigated anticancer compounds and for determination of the most important parameters controlling these properties.

2. Results and discussion

2.1. Chemistry

A synthetic pathway for the preparation of new dispiroindole derivatives **4** is depicted in Scheme 1, and it is based on the previously described methods [32–35,44]. It consists of a 1,3-dipolar cycloaddition reaction of azomethine ylides, (generated in situ via a decarboxylative condensation of isatin derivatives **2** with sarcosine **3**) with bis(α,β-unsaturated) ketones **1** in refluxing ethanol. The reaction commences with a nucleophilic attack of the amino group of sarcosine **3** on the 3-carbonyl function of indole derivative **2**, followed by dehydration to form spiro-oxazalidinone **A**. This, under the reaction conditions expels carbon dioxide to generate a reactive, non-stabilized azomethine ylide **B**, that undergoes in situ 1,3-dipolar addition to 2*E*,6*E*-bis(arylidene)-1-cyclohexanones **1**. The latter process is completely regioselective and affords dispiroindoles **4** as the sole reaction products (TLC analysis). Structures of the isolated products **4a**–**u** were assigned as 4′-aryl-3-(arylmethylidene)-1″-[(cyclic-amino)methylene]-1′-methyl-dispiro [cyclohexane-1,3′-pyrrolidine-2′,3″-[3*H*]indole]-2,2″(1″*H*)-diones based on their spectroscopic (IR, ^{1}H, ^{13}C NMR, MS) and elemental analysis data (Scheme 1).

Single crystal X-ray studies of one member of compounds of type **4** (dispiroindole **4a**) provided a conclusive evidence for the assigned structures (Fig. 2). Specifically, presence of a pyrrolidine ring linking the indole and cyclohexanone moieties via two spiro systems became apparent and stereochemistry at the three chiral centers as depicted in Scheme 1, was revealed (1*S*, 2′*S*, 4′*S*). In addition, the *N*-methylpyrrolidinyl nucleus in **4a** appeared as almost perfect planar pentagonal structure, the cyclohexyl ring as a distorted chair, and the exocyclic olefinic linkage attached to *C*-3 of the cyclohexyl moiety preserved an *E*-form configuration (for additional structural features of **4a** derived from X-ray studies, see Table 1 in the Supplementary material).

The assigned structures are also consistent with the spectral data obtained. For example, a representative to the family compound **4a** exhibited in its IR spectrum a strong stretching vibration bands at ν = 1709 and 1674 cm^{-1} assigned to the carbonyls of ketonic and amidic functions. ^{1}H NMR spectrum of **4a** revealed the pyrrolidinyl methylene protons H_2C-5′, as diastereotopic 2 spin system, that appeared as two triplets at δ_H = 3.47 and 3.96 ppm due to mutual coupling with each other, and in addition to coupling with the vicinal pyrrolidinyl methine proton *HC*-4′ (appeared as a doublet of doublets at δ_H = 4.87 ppm). Further, the methylene protons attached to the indolyl *N*-1″ also appeared as diastereotopic protons (two doublets at δ_H = 4.29 and 4.50 ppm). ^{13}C NMR spectrum of **4a** exhibited the cyclohexyl methylene carbons *C*-6, *C*-5 and *C*-4 at δ_C = 19.0, 28.2, and 30.8 ppm, respectively. The pyrrolidinyl *HC*-4′, H_2C-5′ carbons were observed at δ_C = 48.2 and 57.1 ppm, respectively, and the piperidinyl carbons showed resonances at δ_C = 24.6 (H_2C-4), 25.4 (H_2C-3/5) and 51.6 (NH_2C-2/6) ppm, respectively. The spiro-carbons *C*-1 (*C*-3′), *C*-2′ (*C*-3″) were revealed in the ^{13}C NMR spectrum at δ_C = 63.2 and 76.1 ppm, respectively, while the oxindolyl *C*-2″ and cyclohexyl *C*-2 carbonyl carbons resonated at δ_C = 175.3 and 201.0 ppm, respectively. ^{13}C NMR spectra of other analogs possessing a (4-morpholinyl)methylene residue attached to the *N*-1″ position, as exemplified by **4e**, exhibited the morpholinyl carbons resonances (NCH_2 and OCH_2) at δ_C = 51.5 and 62.4 ppm, respectively. For compound **4k**, the piperazinyl carbons resonance (NH_2C-2/6, NH_2C-3/5) at δ_C = 51.2 and 55.0 ppm (respectively), and the piperazinyl NCH_3 group at δ_C = 46.2 ppm, were observed. Mass spectrum (EI, 70 eV) of **4a** as a representative example of the synthesized compounds, did not show the molecular peak, however, a peak due to elimination of the (cyclic-amino)methylene residue, was detected. For additional spectral data, see the Experimental section.

In contradistinction to the reactions described above, a condensation involving isatin **2a** (X = CH_2), sarcosine **3** and bis(α,β-unsaturated) ketone **1b** (R = 4-ClC_6H_4) under the same conditions afforded compound **5a** (R = 4-ClC_6H_4), instead of the expected corresponding dispiroindole of type **4**. The same course of the reaction was observed for the analogous condensations of isatins **2a** (X = CH_2) or **2c** (X = NCH_3) involving ketone **1c** (R = 2,4-$Cl_2C_6H_3$) that furnished in both instances **5b** (R = 2,4-$Cl_2C_6H_3$) as a sole product (Scheme 1). Mechanistic aspects of the reactions leading to **5** are unclear at the moment, but it seems that the observed loss of the (cyclic-amino)methylene moiety during the course of the reaction can be attributed to an electronic interplay between electron withdrawing substituents R in ketone **1** and X group/atom in isatin **2**. No attempts were made on this occasion to clarify this issue.

2.2. Antitumor properties

The synthesized compounds, **4a**–**u** and **5b**, were screened for their antitumor activity against HEPG2 (liver), HELA (cervical), and PC3 (prostate) human tumor cell lines utilizing the in-vitro Sulfo-Rhodamine-B (SRB) standard method [34,35,45]. From the results obtained (Table 1 and Figs. 1–3 in the Supplementary material), it is apparent that most of the synthesized analogs exhibit mild antitumor properties against the human tumor cell lines tested, however, three of the compounds revealed potent and promising

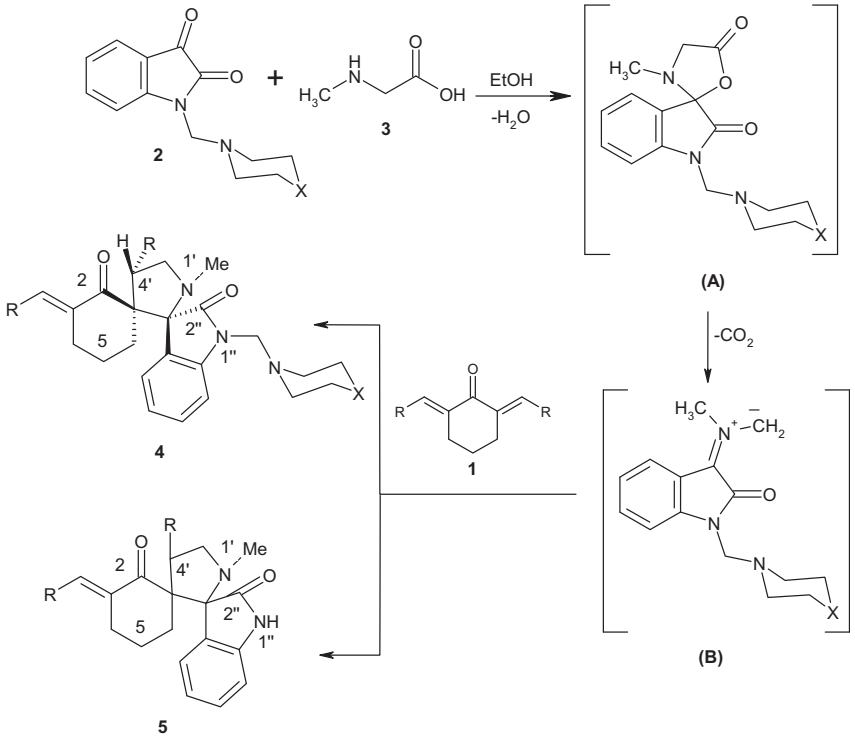

1a, R = Ph
1b, R = 4-ClC_6H_4
1c, R = 2,4-$Cl_2C_6H_3$
1d, R = 4-FC_6H_4
1e, R = 4-$H_3CC_6H_4$
1f, R = 4-$H_3COC_6H_4$
1g, R = 3,4-$(H_3CO)_2C_6H_3$
1h, R = 2-thienyl
1i, R = 5-methyl-2-furanyl

2a, X = CH_2
2b, X = O
2c, X = NCH_3

5a, R = 4-ClC_6H_4
5b, R = 2,4-$Cl_2C_6H_3$

4a; R = Ph, X = CH_2
4b; R = Ph, X = O
4c; R = Ph, X = NMe
4d; R = 4-ClC_6H_4, X = NMe
4e; R = 2,4-$Cl_2C_6H_3$, X = O
4f; R = 4-FC_6H_4, X = CH_2
4g; R = 4-FC_6H_4, X = O
4h; R = 4-FC_6H_4, X = NMe
4i; R = 4-$H_3CC_6H_4$, X = CH_2
4j; R = 4-$H_3CC_6H_4$, X = O
4k; R = 4-$H_3CC_6H_4$, X = NMe
4l; R = 4-$H_3COC_6H_4$, X = CH_2
4m; R = 4-$H_3COC_6H_4$, X = O
4n; R = 4-$H_3COC_6H_4$, X = NMe
4o; R = 3,4-$(H_3CO)_2C_6H_3$, X = CH_2
4p; R = 3,4-$(H_3CO)_2C_6H_3$, X = O
4q; R = 3,4-$(H_3CO)_2C_6H_3$, X = NMe
4r; R = 2-thienyl, X = CH_2
4s; R = 2-thienyl, X = O
4t; R = 2-thienyl, X = NMe
4u; R = 5-methyl-2-furanyl, X = O

Scheme 1. Synthetic routes towards dispiro[cyclohexane-1,3′-pyrrolidine-2′,3″-[3*H*]indoles].

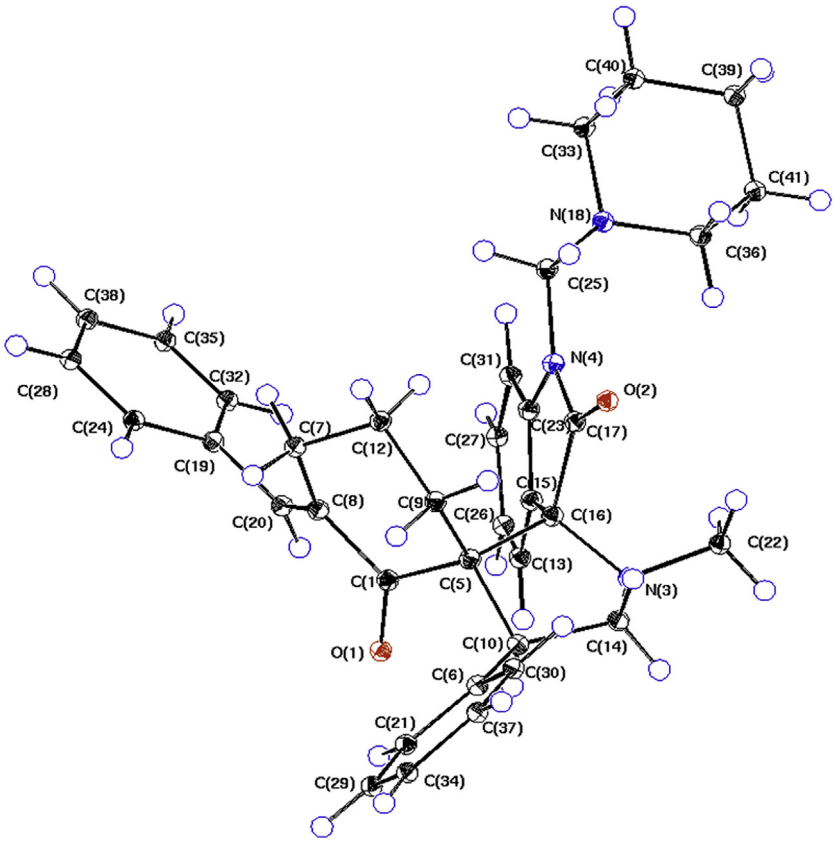

Fig. 2. ORTEP projection of single crystal X-ray diffraction of compound **4a**.

antitumor properties. These are dispiroindole derivatives **4d** and **4p** (IC_{50} = 7.42, 6.99 μM, respectively; reference: Doxorubicin, IC_{50} = 7.36 μM) that showed distinguished antitumor activity against HEPG2 (liver) human tumor cell line, and dispiroindole **4g** (IC_{50} = 6.96 μM; reference: Doxorubicin, IC_{50} = 7.71 μM) that emerged as potent antitumor agent against HELA (cervical) cell line (Table 1).

In order to understand the observed pharmacological properties of the investigated dispiroindole analogs and determine the crucial factors governing these activities, QSAR studies were undertaken.

Table 1
Antitumor properties of the synthesized compounds **4a**–**u**, **5b**.

Entry	Compd.	R	X	IC_{50}, μg/ml (μM)[a]		
				HEPG2 (liver)	HELA (cervical)	PC3 (prostate)
1	**4a**	Ph	CH_2	10.17 (18.64)	6.32 (11.58)	17.25 (31.61)
2	**4b**	Ph	O	7.31 (13.35)	8.13 (14.84)	14.63 (26.71)
3	**4c**	Ph	NMe	11.10 (19.79)	14.07 (25.09)	32.46 (57.89)
4	**4d**	4-ClC_6H_4	NMe	4.67 (7.42)	7.47 (11.86)	11.00 (17.47)
5	**4e**	2,4-$Cl_2C_6H_3$	O	17.06 (24.89)	15.28 (22.29)	15.00 (21.88)
6	**4f**	4-FC_6H_4	CH_2	10.00 (17.19)	8.83 (15.18)	11.67 (20.06)
7	**4g**	4-FC_6H_4	O	4.72 (8.09)	4.06 (6.96)	11.38 (19.50)
8	**4h**	4-FC_6H_4	NMe	7.53 (12.62)	9.51 (15.94)	10.83 (18.15)
9	**4i**	4-$H_3CC_6H_4$	CH_2	9.39 (16.36)	11.25 (19.61)	18.33 (31.95)
10	**4j**	4-$H_3CC_6H_4$	O	12.50 (21.71)	7.64 (13.27)	18.95 (32.91)
11	**4k**	4-$H_3CC_6H_4$	NMe	11.32 (19.23)	12.50 (21.23)	15.73 (26.72)
12	**4l**	4-$H_3COC_6H_4$	CH_2	15.00 (24.76)	9.78 (16.14)	25.34 (41.83)
13	**4m**	4-$H_3COC_6H_4$	O	11.39 (18.74)	11.22 (18.46)	35.75 (58.82)
14	**4n**	4-$H_3COC_6H_4$	NMe	12.50 (20.14)	9.07 (14.61)	11.33 (18.25)
15	**4o**	3,4-$(H_3CO)_2C_6H_3$	CH_2	17.53 (26.33)	12.50 (18.77)	25.59 (38.43)
16	**4p**	3,4-$(H_3CO)_2C_6H_3$	O	4.67 (6.99)	7.28 (10.90)	21.39 (32.03)
17	**4q**	3,4-$(H_3CO)_2C_6H_3$	NMe	8.33 (12.23)	11.11 (16.32)	13.58 (19.95)
18	**4r**	2-Thienyl	CH_2	14.17 (25.40)	5.99 (10.74)	12.10 (21.69)
19	**4s**	2-Thienyl	O	16.77 (29.96)	15.33 (27.39)	16.83 (30.07)
20	**4t**	2-Thienyl	NMe	5.67 (9.90)	7.89 (13.77)	16.95 (29.59)
21	**4u**	5-Methyl-2-furanyl	O	15.77 (28.38)	10.00 (18.00)	11.75 (21.15)
22	**5b**	2,4-$Cl_2C_6H_3$	–	9.61 (16.39)	13.00 (22.17)	15.00 (25.58)
23	Doxorubicin	–	–	4.00 (7.36)	4.19 (7.71)	4.80 (8.83)

[a] IC_{50} = concentration required to produce 50% inhibition of cell growth compared to control experiment.

2.3. QSAR study

The QSAR study was performed using Discovery Studio 2.5 software (Accelrys Inc., San Diego, CA, USA). A set of 20 synthesized dispiro[cyclohexane-1,3′-pyrrolidine-2′,3″-[3*H*]indoles] was used as a training set for the present QSAR modeling. The two remaining synthesized analogs were used as an external test set to assess the predictive power of the resulting QSAR models and validate the established ones. The test sets of the analogs were selected to display variable potential pharmacological properties representing potent and mild antitumor activity.

2.3.1. QSAR modeling

Many molecular descriptors were calculated for each compound employing a calculated molecular properties module. The 3D structures of the training set analogs were imported into the Discovery Studio to calculate various molecular descriptors for each antitumor active agent. 2D Descriptors involved: AlogP, fingerprints, molecular properties, surface area, volume and topological descriptors, and the 3D descriptors: dipole, jurs descriptors, principle moments of inertia and shadow indices. Furthermore, the training set compounds were fitted (using the best-fit option) against representative pharmacophores and their fit values were added as additional descriptors. The fit values of the training set compounds were calculated automatically using the Discovery Studio software. Moreover, energies of highest occupied and lowest unoccupied molecular orbitals (HOMO and LUMO) [35] of each of the training set compounds were determined using this software and imported as additional descriptors. Multiple linear regression (MLR) analysis were employed to search for optimal QSAR models that combine high quality binding pharmacophores with other molecular descriptors and being capable of correlating bioactivity variation across the used training set collection. QSAR models were validated employing leave one-out cross-validation, r^2 (squared correlation coefficient value) and $r^2_{\text{prediction}}$ (predictive squared correlation coefficient value) [35]. Statistical outliers were identified from experimental versus predicted plots.

Equations (1)–(3) represent our best performing QSAR models (Figs. 3–5 show the corresponding scatter plots of the experimental versus estimated bioactivity values for the training set compounds, against HEPG2, HELA, and PC3 tumor cell lines, respectively; Tables 2–4 summarize the estimated activity data of the training set analogs and the calculated descriptors governing activity according to the optimized QSAR models for the training set compounds against HEPG2, HELA, and PC3 tumor cell lines, respectively).

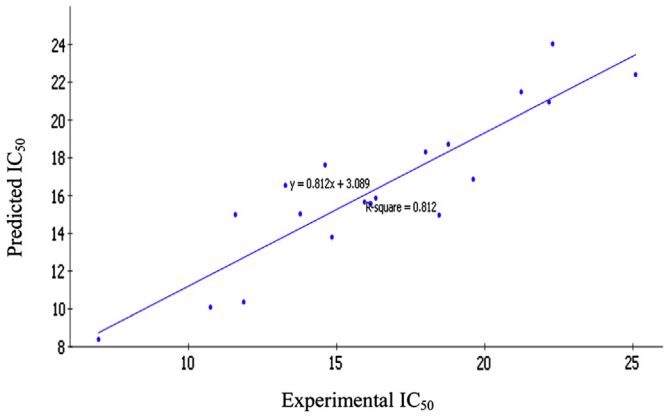

Fig. 4. Predicted versus experimental IC_{50} values of the training set compounds against HELA (cervical) human tumor cell line according to Equation (2).

Equation (1)

Potency (IC_{50}) (a concentration required to produce 50% inhibition of cell growth compared to the control experiment) against HEPG2 (liver) human tumor cell line ($N = 19$, $r^2 = 0.903$, $r^2_{\text{adjusted}} = 0.855$, $r^2_{\text{prediction}} = 0.773$) "compound **5b** was identified as a statistical outlier".

$$IC_{50} = 2919.1 - 9.7865 \text{ Num atom classes} + 0.062149 \text{ Jurs WNSA } 2 - 269.96 \text{ Shadow Zlength} \quad (1)$$

Equation (2)

Potency (IC_{50}) against HELA (cervical) human tumor cell line ($N = 19$, $r^2 = 0.812$, $r^2_{\text{adjusted}} = 0.739$, $r^2_{\text{prediction}} = 0.605$) "compound **4s** was identified as a statistical outlier".

$$IC_{50} = -559.06 - 2.902 \text{ Num chains} + 17.125 \text{ Kappa-1} + 65.381 \text{ Rad of gyration} \quad (2)$$

Equation (3)

Potency (IC_{50}) against PC3 (prostate cancer) cell line ($N = 20$, $r^2 = 0.848$, $r^2_{\text{adjusted}} = 0.672$, $r^2_{\text{prediction}} = 0.632$)

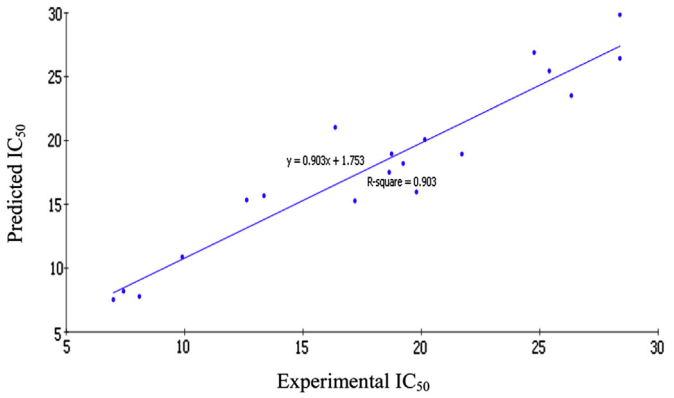

Fig. 3. Predicted versus experimental IC_{50} values of the training set compounds against HEPG2 (liver) human tumor cell line according to Equation (1).

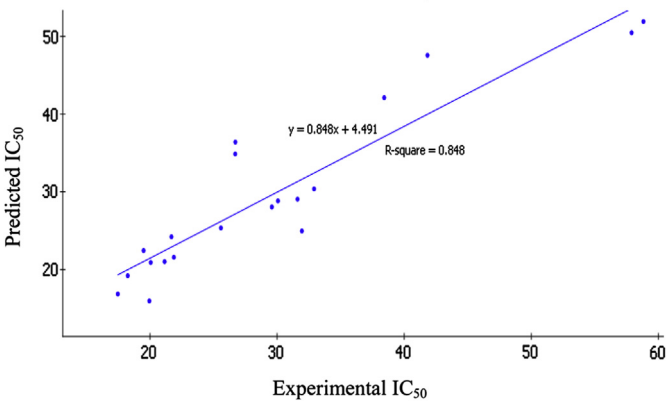

Fig. 5. Predicted versus experimental IC_{50} values of the training set compounds against PC3 (prostate) human tumor cell line according to Equation (3).

Table 2
Estimated activity data of the training set analogs against HEPG2 (liver) human tumor cell line and calculated descriptors governing activity according to Equation (1).[a]

Compd.	Observed activity	Estimated activity	Residual	Num atom classes	Jurs WNSA 2	Shadow Zlength
4a	18.64	17.4737	1.1663	35	−428.068	9.3810
4b	13.35	13.6051	−0.2551	35	−481.628	9.3830
4c	19.79	15.7371	4.0529	36	−476.637	9.3400
4d	7.42	8.0799	−0.6599	38	−761.416	9.2303
4f	17.19	16.3916	0.7984	37	−944.997	9.1935
4g	8.09	8.2794	−0.1894	37	−612.481	9.3001
4h	12.62	14.5779	−1.9579	38	−679.884	9.225
4i	16.36	20.7767	−4.4167	37	−454.833	9.2901
4j	21.71	19.4638	2.2462	37	−515.486	9.2810
4k	19.23	18.6804	0.5496	38	−505.279	9.2500
4l	24.76	26.0730	1.3130	39	−576.795	9.1699
4m	18.74	19.1274	−0.3874	39	−645.113	9.1799
4n	20.14	20.1415	−0.0015	40	−648.989	9.1390
4o	26.33	22.9963	3.3337	47	−667.944	8.8703
4p	6.99	7.4965	−0.5065	47	−744.893	8.9100
4r	25.40	25.4954	−0.0.954	37	−408.443	9.2833
4s	29.96	26.6566	3.3033	37	−464.906	9.2660
4t	9.90	10.1045	−0.2045	38	−473.861	9.2890
4u	28.38	29.2569	−0.8769	39	−407.850	9.1970

[a] Compound **5b** was identified as a statistical outlier.

$$IC_{50} = -426.14 + 46.082\ \text{Kappa-1AM} + 20.912\ \text{Dipole X} - 514.2\ \text{Jurs RNCG} \quad (3)$$

Abbreviations used: Num atom classes, are different atom classes from symmetry perception (excluding hydrogens), for example, benzene would have a value "1" and toluene would have a value "5"; Jurs WNSA 2, is the surface-weighted charged partial surface areas "set of six descriptors obtained by multiplying descriptors 1 to 6 by the total molecular solvent-accessible surface area and dividing by 1000"; Shadow Zlength, is the length of molecule in the *Z* dimension; Num chains, is the unbranched chains needed to cover all the non-ring bonds in the molecule; Kappa-1, is the shape index of order one; Rad of gyration, is the radius of gyration; Kappa-1AM, is the alpha-modified shape index of order one; Dipole X, the 3D electronic descriptors that indicates the strength and orientation behavior of a molecule in an electrostatic field, both the magnitude and the components (X, Y, Z) of the dipole moment are calculated (Debyes), it is estimated by utilizing partial atomic charges and atomic coordinates, partial atomic charges are computed using Gasteiger if not present, dipole properties have been correlated to long range ligand–receptor recognition and subsequent binding; Jurs RNCG (Relative Negative Charge), is the charge of most negative atom divided by the total negative charge.

Table 3
Estimated activity data of the training set analogs against HELA (cervical) human tumor cell line and calculated descriptors governing activity according to Equation (2).[a]

Compd.	Observed activity	Estimated activity	Residual	Num chains	Kappa-1	Rad of gyration
4a	11.58	14.4213	−2.841	45	29.6967	2.9904
4b	14.84	13.7265	1.114	43	29.6967	2.8910
4c	25.09	22.184	2.906	47	30.6432	2.9500
4d	11.86	11.557	0.303	47	32.5424	2.2900
4e	22.29	23.784	−1.494	43	33.4948	2.0500
4g	6.96	8.2591	−1.299	43	31.5918	2.3110
4h	15.94	15.5453	0.395	47	32.5424	2.3510
4i	19.61	16.4259	3.184	51	31.5918	2.7910
4j	13.27	15.626	−2.356	49	31.5918	2.6900
4k	21.23	21.605	−0.375	53	32.5424	2.7100
4l	16.14	15.605	0.535	51	33.4948	2.2800
4m	18.46	15.525	2.935	49	33.4948	2.1900
4n	14.61	17.512	−2.902	53	34.4490	2.1480
4o	18.77	17.950	0.82	57	37.3210	1.5800
4q	16.32	16.298	0.022	59	38.2812	1.3920
4r	10.74	10.176	0.564	41	27.8104	3.2420
4t	13.77	15.274	−1.504	43	28.7524	3.1620
4u	18.00	18.383	−0.383	45	29.6967	3.051
5b	22.17	21.171	0.999	33	28.1352	2.970

[a] Compound **4s** was identified as a statistical outlier.

Table 4
Estimated activity data of the training set analogs against PC3 (prostate) human tumor cell line and calculated descriptors governing activity according to Equation (3).

Compd.	Observed activity	Estimated activity	Residual	Kappa-1AM	Dipole X	Jurs RNCG
4a	31.61	29.406	2.204	26.3646	0.07785	1.480
4b	26.71	28.7558	−2.0458	26.3272	−0.11669	1.470
4c	57.89	49.898	7.992	27.2651	0.54876	1.540
4d	17.47	16.547	0.923	29.6967	1.29188	1.853
4e	21.88	21.675	0.205	31.1932	1.28846	1.977
4f	20.06	20.116	−0.056	28.1115	1.21826	1.701
4g	19.50	22.098	−2.598	28.0739	1.05165	1.687
4i	31.95	25.506	6.444	28.2434	0.05429	1.655
4j	32.91	30.521	2.389	28.2057	−0.11464	1.635
4k	26.72	36.309	−9.589	29.1487	0.54302	1.735
4l	41.83	47.385	−5.555	30.0561	1.40904	1.830
4m	58.82	52.856	5.964	30.0183	1.26220	1.810
4n	18.25	19.302	−1.052	30.9655	0.66858	1.936
4o	38.43	42.549	−4.119	33.7809	0.69063	2.144
4q	19.95	15.984	3.966	34.6973	0.20402	2.258
4r	21.69	24.234	−2.544	25.3919	−1.09960	1.355
4s	30.07	28.239	1.831	25.3546	−1.31764	1.335
4t	29.59	28.205	1.385	26.2897	−1.58491	1.408
4u	21.15	21.1157	−0.0342	26.4396	−2.08210	1.415
5b	25.58	25.604	−0.024	25.9122	0.64708	1.470

2.3.2. Validation of QSAR

External validation of the determined QSAR models was performed utilizing two of our synthesized analogs exhibiting potent and mild antitumor properties against the tested tumor cell lines. The observed activities and those provided by QSAR studies were presented in Table 5. It should be noted that the predicated antitumor activities by our QSAR models were very close to those experimentally observed, indicating that these models can be safely applied for predication of more effective hits having the same skeletal framework as that of the potent antitumor compound.

3. Conclusion

A variety of 4′-aryl-3-(arylmethylidene)-1″-[(cyclic-amino) methylene]-1′-methyl-dispiro[cyclohexane-1,3′-pyrrolidine-2′,3″-[3*H*]indole]-2,2″(1″*H*)-diones **4a**–**u** were prepared via a 1,3-dipolar cycloaddition reaction of 2*E*,6*E*-bis(arylidene)-1-cyclohexanones **1a**–**i**, with azomethine ylides generated in situ via a decarboxylative condensation of isatins **2a**–**c** and sarcosine (**3**). It was observed that certain combinations of the reactants **1** and **2** (reaction of **1b** with **2a**, and **1c** with **2a** or **2c**) did not afford the expected dispiroindoles **4**, but instead the corresponding dealkylated dispiroindoles **5**. Single crystal X-ray study of **4a** provided support for the assigned structures and stereochemistry of the chiral centers in dispiroindoles **4**. The synthesized compounds were screened for their antitumor properties against HEPG2 (liver), HELA (cervical), and PC3 (prostate) human tumor cell lines utilizing the in-vitro Sulfo-Rhodamine-B (SRB) standard method. Most of the synthesized analogs exhibited mild antitumor properties against the tested human tumor cell lines, however, three of the compounds, **4d** and **4p** (active against HEPG2), and compound **4g** (active against

Table 5
External validation for the established QSAR models.

Cell lines	Compd.	Experimental activity (IC_{50}, μM)	Predicted activity (IC_{50}, μM)	Descriptors								
				Num atom classes	Jurs WNSA 2	Shadow Zlength	Num chains	Kappa-1	Rad of gyration	Kappa 1AM	Dipole X	Jurs RNCG
HEPG2	**4e**	24.89	26.081	43	−944.997	8.9401	–	–	–	–	–	–
	4q	12.23	12.558	48	−744.893	8.855	–	–	–	–	–	–
HELA	**4f**	15.18	14.747	–	–	–	45	31.5918	2.4990	–	–	–
	4p	10.90	9.973	–	–	–	55	34.3210	2.1550	–	–	–
PC3	**4h**	18.15	21.922	–	–	–	–	–	–	29.0165	1.72002	1.799
	4p	32.03	34.2814	–	–	–	–	–	–	33.7427	−1.51388	2.067

HELA) demonstrate rather high anticancer activity, close or even better than that of the reference standard Doxorubicin. Finally, the QSAR studies revealed good predictive and statistically significant 3 descriptor models (r^2 = 0.903–0.812, $r^2_{adjusted}$ = 0.855–0.672, $r^2_{prediction}$ = 0.773–0.605) for the investigated compounds.

4. Experimental

Melting points were determined on an Electrothermal Stuart SMP3 melting point apparatus. IR spectra (KBr) were recorded on a Shimadzu FT-IR 8400S spectrophotometer. NMR spectra were recorded on a Varian MERCURY 300 (^{1}H: 300, ^{13}C: 75 MHz) spectrometer, and the mass spectra, a Shimadzu GCMS-QP 1000 EX (EI, 70 eV) spectrometer, was used. The starting materials **1a**–**i** [46–49] and **2a**–**c** [50,51] were prepared according to the previously reported procedures (Figs. 4–7 of Supplementary material exhibit representative examples of the spectral features of the synthesized compounds).

*4.1. Synthesis of 4′-aryl-3-(arylmethylidene)-1″-[(cyclic-amino) methylene]-1′-methyl-dispiro[cyclohexane-1,3′-pyrrolidine-2′,3″-[3H]indole]-2,2″(1″H)-diones **4a**–**u** and 4′-aryl-3-(arylmethylidene)-1′-methyl-dispiro[cyclohexane-1,3′-pyrrolidine-2′,3″-[3H]indole]-2,2″(1″H)-diones **5a**,**b** (general procedure)*

A mixture of equimolar amounts of 2,6-bis(arylidene)-1-cyclohexanone **1a**–**i** (5 mmol), the corresponding isatin **2a**–**c** and sarcosine (**3**) in absolute ethanol (25 ml) was boiled under reflux for the appropriate time. The separated solid while refluxing was collected and crystallized from a suitable solvent affording the corresponding **4a**–**k**,**r**,**s**. In case of compounds **4l**–**q**,**t**,**u** the reaction mixture was concentrated to half of its initial volume and stored at room temperature overnight so, the separated solid was collected and crystallized from a suitable solvent affording the corresponding analogs. In case of reaction of **1b** with **2a** and reaction of **1c** with either **2a** or **2c** under the same previously described procedure, the corresponding **5a**,**b** were isolated.

*4.1.1. 1′-Methyl-4′-phenyl-3-(phenylmethylidene)-1″-[(1-piperidinyl) methylene]-dispiro[cyclohexane-1,3′-pyrrolidine-2′,3″-[3H]indole]-2,2″(1″H)-dione (**4a**)*

Obtained from of **1a**, **2a** and **3**. Reaction time 24 h, colorless crystals from ethanol, mp 175–176 °C, yield (1.88 g) 69%. IR: ν_{max}/cm^{-1} 1709, 1674 (C=O), 1609, 1485. ^{1}H NMR ($CDCl_3$): δ 1.11–1.53 (m, 10H, cyclohexyl 4H + piperidinyl 3CH_2), 2.09 (s, 3H, pyrrolidinyl NCH_3), 2.15–2.23 (m, 1H, cyclohexyl H), 2.41 (br d, 1H, cyclohexyl H), 2.57 (br s, 4H, piperidinyl 2NCH_2), 3.47 (t, 1H, upfield H of pyrrolidinyl CH_2CH, J = 8.40 Hz), 3.96 (t, 1H, downfield H of pyrrolidinyl CH_2CH, J = 9.75 Hz), 4.29 (d, 1H, upfield H of NCH_2N, J = 12.90 Hz), 4.50 (d, 1H, downfield H of NCH_2N, J = 12.90 Hz), 4.87 (dd, 1H, pyrrolidinyl CHCH$_2$, J = 8.10, 9.90 Hz), 6.88–7.53 (m, 15H, 14 arom. H + olefinic CH). ^{13}C NMR (DMSO-d_6): δ 19.0 (cyclohexyl *C*-6), 23.6 (piperidinyl H_2C-4), 25.4 (piperidinyl H_2C-3/5), 28.2 (cyclohexyl *C*-5), 30.8 (cyclohexyl *C*-4), 34.1 (pyrrolidinyl NCH_3), 48.2 (HC-4′), 51.6 (piperidinyl NCH_2-2/6), 57.1 (H_2C-5′), 61.9 (NCH_2N), 63.2 [spiro *C*-1 (*C*-3′)], 76.1 [spiro *C*-2′ (*C*-3″)], 109.5, 122.1, 125.2, 126.6, 127.7, 128.1, 128.3, 128.7, 129.1, 129.6, 129.8, 130.2, 135.2, 136.3, 137.3, 139.3, 144.3 (arom. *C* + olefinic *C*), 175.3 [oxindolyl *C*=O (*C*-2″)], 201.0 [cyclohexyl *C*=O (*C*-2)].MS: *m*/*z* (%) 447 [(M − $C_6H_{12}N$), 63]. Anal. Calcd. for $C_{36}H_{39}N_3O_2$ (545.73): C, 79.23; H, 7.20; N, 7.70. Found: C, 79.29; H, 7.24; N, 7.82.

*4.1.2. 1′-Methyl-1″-[(4-morpholinyl)methylene]-4′-phenyl-3-(phenylmethylidene)-dispiro[cyclohexane-1,3′-pyrrolidine-2′,3″-[3H]indole]-2,2″(1″H)-dione (**4b**)*

Obtained from **1a**, **2b** and **3**. Reaction time 27 h, colorless crystals from ethanol, mp 191–192 °C, yield (2.10 g) 77%. IR: ν_{max}/cm^{-1} 1709, 1674 (C=O), 1609, 1485. ^{1}H NMR ($CDCl_3$): δ 1.12–1.33 (m, 4H, cyclohexyl H), 2.09 (s, 3H, pyrrolidinyl NCH_3), 2.15–2.23 (m, 1H, cyclohexyl H), 2.40 (br d, 1H, cyclohexyl H), 2.61 (t, 4H, morpholinyl 2NCH_2, J = 4.65 Hz), 3.47 (t, 1H, upfield H of pyrrolidinyl CH_2CH, J = 8.25 Hz), 3.65 (t, 4H, morpholinyl 2OCH_2, J = 4.50 Hz), 3.95 (t, 1H, downfield H of pyrrolidinyl CH_2CH, J = 9.75 Hz), 4.33 (d, 1H, upfield H of NCH_2N, J = 13.20 Hz), 4.48 (d, 1H, downfield H of NCH_2N, J = 12.90 Hz), 4.87 (dd, 1H, pyrrolidinyl CHCH$_2$, J = 7.50, 10.50 Hz), 6.86–7.51 (m, 15H, 14 arom. H + olefinic CH). MS: *m*/*z* (%) 447 [(M − $C_5H_{10}NO$), 23]. Anal. Calcd. for $C_{35}H_{37}N_3O_3$ (547.70): C, 76.76; H, 6.81; N, 7.67. Found: C, 76.74; H, 6.88; N, 7.79.

*4.1.3. 1′-Methyl-1″-[(4-methylpiperazin-1-yl)methylene]-4′-phenyl-3-(phenylmethylidene)-dispiro[cyclohexane-1,3′-pyrrolidine-2′,3″-[3H]indole]-2,2″(1″H)-dione (**4c**)*

Obtained from **1a**, **2c** and **3**. Reaction time 28 h, almost colorless crystals from ethanol, mp 176–178 °C, yield (1.77 g) 63%. IR: ν_{max}/cm^{-1} 1697, 1670 (C=O), 1593, 1566. ^{1}H NMR ($CDCl_3$): δ 1.10–1.32 (m, 4H, cyclohexyl H), 2.09 (s, 3H, pyrrolidinyl NCH_3), 2.15–2.29 (m, 5H, 2 cyclohexyl H + piperazinyl NCH_3), 2.38 (br s, 4H, piperazinyl 2NCH_2), 2.65 (br s, 4H, piperazinyl 2NCH_2), 3.47 (t, 1H, upfield H of pyrrolidinyl CH_2CH, J = 8.55 Hz), 3.95 (t, 1H, downfield H of pyrrolidinyl CH_2CH, J = 9.75 Hz), 4.35 (d, 1H, upfield H of NCH_2N, J = 12.90 Hz), 4.46 (d, 1H, downfield H of NCH_2N, J = 12.60 Hz), 4.87 (dd, 1H, pyrrolidinyl CHCH$_2$, J = 7.80, 10.80 Hz), 6.85–7.51 (m, 15H, 14 arom. H + olefinic CH). Anal. Calcd. for $C_{36}H_{40}N_4O_2$ (560.75): C, 77.11; H, 7.19; N, 9.99. Found: C, 77.08; H, 7.28; N, 10.13.

*4.1.4. 4′-(4-Chlorophenyl)-3-[(4-chlorophenyl)methylidene]-1′-methyl-1″-[1-(4-methylpiperazinyl)methylene]-dispiro[cyclohexane-1,3′-pyrrolidine-2′,3″-[3H]indole]-2,2″(1″H)-dione (**4d**)*

Obtained from **1b**, **2c** and **3**. Reaction time 29 h, colorless crystals from ethanol, mp 176–178 °C, yield (2.12 g) 67%. IR: ν_{max}/cm^{-1} 1694, 1670 (C=O), 1593, 1489. ^{1}H NMR ($CDCl_3$): δ 1.10–1.35 (m, 4H, cyclohexyl H), 2.07 (s, 3H, pyrrolidinyl NCH_3), 2.13–2.22 (m, 1H, cyclohexyl H) 2.33–2.36 (m, 4H, cyclohexyl H + piperazinyl NCH_3), 2.55 (br s, 4H, piperazinyl 2NCH_2), 2.75 (br s, 4H, piperazinyl

2NCH$_2$), 3.44 (t, 1H, upfield H of pyrrolidinyl *CH*$_2$CH, J = 8.40 Hz), 3.86 (t, 1H, downfield H of pyrrolidinyl *CH*$_2$CH, J = 9.75 Hz), 4.36 (d, 1H, upfield H of NC*H*$_2$N, J = 12.60 Hz), 4.49 (d, 1H, downfield H of NC*H*$_2$N, J = 12.90 Hz), 4.81 (dd, 1H, pyrrolidinyl *CH*CH$_2$, J = 7.80, 10.50 Hz), 6.84–7.44 (m, 13H, 12 arom. H + olefinic CH). Anal. Calcd. for $C_{36}H_{38}Cl_2N_4O_2$ (629.64): C, 68.67; H, 6.08; N, 8.90. Found: 68.72; H, 6.12; N, 9.04.

4.1.5. 4′-(2,4-Dichlorophenyl)-3-[(2,4-dichlorophenyl)methylidene]-1′-methyl-1″-[(4-morpholinyl)methylene]-dispiro[cyclohexane-1,3′-pyrrolidine-2′,3″-[3H]indole]-2,2″(1″H)-dione (**4e**)

Obtained from **1c**, **2b** and **3**. Reaction time 24 h, colorless crystals from ethanol, mp 227–229 °C, yield (2.37 g) 69%. IR: ν_{max}/cm^{-1} 1709, 1682 (C=O), 1609, 1597. ^{1}H NMR (CDCl$_3$): δ 1.04–1.33 (m, 4H, cyclohexyl H), 1.91–2.00 (m, 1H, cyclohexyl H), 2.06 (s, 3H, pyrrolidinyl NCH$_3$), 2.23 (br s, 1H, cyclohexyl H), 2.56–2.65 (m, 4H, morpholinyl 2NCH$_2$), 3.51 (t, 1H, upfield H of pyrrolidinyl *CH*$_2$CH, J = 9.30 Hz), 3.66 (t, 4H, morpholinyl 2OCH$_2$, J = 4.65 Hz), 3.96 (t, 1H, downfield H of pyrrolidinyl *CH*$_2$CH, J = 9.30 Hz), 4.30 (d, 1H, upfield H of NC*H*$_2$N, J = 12.60 Hz), 4.53 (d, 1H, downfield H of NC*H*$_2$N, J = 12.60 Hz), 5.11 (t, 1H, pyrrolidinyl *CH*CH$_2$, J = 8.40 Hz), 6.74–8.01 (m, 11H, 10 arom. H + olefinic CH). ^{13}C NMR (CDCl$_3$): δ 19.3 (cyclohexyl *C*-6), 28.5 (cyclohexyl *C*-5), 31.1 (cyclohexyl *C*-4), 35.0 (pyrrolidinyl NCH$_3$), 45.2 (H*C*-4′), 51.5 (morpholinyl NCH$_2$), 57.5 (H$_2$*C*-5′), 62.3 (NCH$_2$N), 62.4 [spiro *C*-1 (*C*-3′)], 66.9 (morpholinyl OCH$_2$), 77.6 [spiro *C*-2′ (*C*-3″)], 109.5, 123.9, 126.7, 127.2, 127.3, 128.4, 128.9, 129.1, 129.7, 129.8, 131.3, 132.4, 132.5, 133.2, 134.9, 135.0, 136.4, 137.0, 138.1, 141.5 (arom. *C* + olefinic *C*), 176.3 [oxindolyl *C*=O (*C*-2″)], 200.3 [cyclohexyl *C*=O (*C*-2)]. MS: m/z (%) 583 [(M − $C_5H_{10}NO$), 5], 585 (5), 587 (4), 589 (1). Anal. Calcd. for $C_{35}H_{33}Cl_4N_3O_3$ (685.48): C, 61.33; H, 4.85; N, 6.13. Found: C, 61.41; H, 4.90; N, 6.27.

4.1.6. 4′-(4-Fluorophenyl)-3-[(4-fluorophenyl)methylidene]-1′-methyl-1″-[(1-piperidinyl)methylene]-dispiro[cyclohexane-1,3′-pyrrolidine-2′,3″-[3H]indole]-2,2″(1″H)-dione (**4f**)

Obtained from reaction of **1d**, **2a** and **3**. Reaction time 20 h, colorless crystals from ethanol, mp 168–170 °C, yield (1.60 g) 55%. IR: ν_{max}/cm^{-1} 1705, 1674 (C=O), 1609, 1508. ^{1}H NMR (CDCl$_3$): δ 1.09–1.55 (m, 10H, cyclohexyl 4H + piperidinyl 3CH$_2$), 2.07 (s, 3H, pyrrolidinyl NCH$_3$), 2.13–2.33 (m, 2H, cyclohexyl H), 2.56 (t, 4H, piperidinyl 2NCH$_2$, J = 5.10 Hz), 3.46 (t, 1H, upfield H of pyrrolidinyl *CH*$_2$CH, J = 8.40 Hz), 3.88 (t, 1H, downfield H of pyrrolidinyl *CH*$_2$CH, J = 9.60 Hz), 4.29 (d, 1H, upfield H of NC*H*$_2$N, J = 12.60 Hz), 4.47 (d, 1H, downfield H of NC*H*$_2$N, J = 12.90 Hz), 4.82 (dd, 1H, pyrrolidinyl *CH*CH$_2$, J = 7.80, 10.20 Hz), 6.89–7.50 (m, 13H, 12 arom. H + olefinic CH). MS: m/z (%) 483 [(M − $C_6H_{12}N$), 37]. Anal. Calcd. for $C_{36}H_{37}F_2N_3O_2$ (581.71): C, 74.33; H, 6.41; N, 7.22. Found: C, 74.35; H, 6.38; N, 7.31.

4.1.7. 4′-(4-Fluorophenyl)-3-[(4-fluorophenyl)methylidene]-1′-methyl-1″-[(4-morpholinyl)methylene]-dispiro[cyclohexane-1,3′-pyrrolidine-2′,3″-[3H]indole]-2,2″(1″H)-dione (**4g**)

Obtained from **1d**, **2b** and **3**. Reaction time 24 h, colorless crystals from ethanol, mp 178–180 °C, yield (1.79 g) 61%. IR: ν_{max}/cm^{-1} 1713, 1682 (C=O), 1605, 1508. ^{1}H NMR (CDCl$_3$): δ 1.12–1.33 (m, 4H, cyclohexyl H), 2.10 (s, 3H, pyrrolidinyl NCH$_3$), 2.18–2.33 (m, 2H, cyclohexyl H), 2.64 (br s, 4H, morpholinyl 2NCH$_2$), 3.52 (t, 1H, upfield H of pyrrolidinyl *CH*$_2$CH, J = 9.00 Hz), 3.68 (t, 4H, morpholinyl 2OCH$_2$, J = 4.65 Hz), 3.88 (dd, 1H, downfield H of pyrrolidinyl *CH*$_2$CH, J = 9.30, 10.20 Hz), 4.38 (d, 1H, upfield H of NC*H*$_2$N, J = 13.20 Hz), 4.51 (d, 1H, downfield H of NC*H*$_2$N, J = 12.60 Hz), 4.82 (t, 1H, pyrrolidinyl *CH*CH$_2$, J = 8.70 Hz), 6.90–7.49 (m, 13H, 12 arom. H + olefinic CH). Anal. Calcd. for $C_{35}H_{35}F_2N_3O_3$ (583.68): C, 72.02; H, 6.04; N, 7.20. Found: C, 72.11; H, 6.08; N, 7.32.

4.1.8. 4′-(4-Fluorophenyl)-3-[(4-fluorophenyl)methylidene]-1′-methyl-1″-[1-(4-methylpiperazinyl)methylene]-dispiro[cyclohexane-1,3′-pyrrolidine-2′,3″-[3H]indole]-2,2″(1″H)-dione (**4h**)

Obtained from **1d**, **2c** and **3**. Reaction time 25 h, colorless crystals from ethanol, mp 201–203 °C, yield (2.49 g) 84%. IR: ν_{max}/cm^{-1} 1697, 1667 (C=O), 1601, 1582. ^{1}H NMR (CDCl$_3$): δ 1.10–1.34 (m, 4H, cyclohexyl H), 2.07 (s, 3H, pyrrolidinyl NCH$_3$), 2.13–2.25 (m, 2H, cyclohexyl H) 2.33 (s, 3H, piperazinyl NCH$_3$), 2.52 (br s, 4H, piperazinyl 2NCH$_2$), 2.74 (br s, 4H, piperazinyl 2NCH$_2$), 3.45 (dd, 1H, upfield H of pyrrolidinyl *CH*$_2$CH, J = 7.80, 9.00 Hz), 3.86 (dd, 1H, downfield H of pyrrolidinyl *CH*$_2$CH, J = 9.15, 10.35 Hz), 4.36 (d, 1H, upfield H of NC*H*$_2$N, J = 12.90 Hz), 4.48 (d, 1H, downfield H of NC*H*$_2$N, J = 12.90 Hz), 4.82 (dd, 1H, pyrrolidinyl *CH*CH$_2$, J = 7.95, 10.35 Hz), 6.85–7.46 (m, 13H, 12 arom. H + olefinic CH). Anal. Calcd. for $C_{36}H_{38}F_2N_4O_2$ (596.73): C, 72.46; H, 6.42; N, 9.39. Found: 72.52; H, 6.39; N, 9.53.

4.1.9. 1′-Methyl-4′-(4-methylphenyl)-3-[(4-methylphenyl)methylidene]-1″-[(1-piperidinyl)methylene]-dispiro[cyclohexane-1,3′-pyrrolidine-2′,3″-[3H]indole]-2,2″(1″H)-dione (**4i**)

Obtained from **1e**, **2a** and **3**. Reaction time 20 h, almost colorless crystals from ethanol, mp 162–164 °C, yield (1.70 g) 59%. IR: ν_{max}/cm^{-1} 1713, 1674 (C=O), 1605, 1500. ^{1}H NMR (CDCl$_3$): δ 1.09–1.53 (m, 10 H, cyclohexyl 4H + piperidinyl 3CH$_2$), 2.07 (s, 3H, pyrrolidinyl NCH$_3$), 2.11–2.26 (m, 1H, cyclohexyl H), 2.32 (s, 3H, ArCH$_3$), 2.34 (s, 3H, ArCH$_3$), 2.41 (br d, 1H, cyclohexyl H), 2.55 (br s, 4H, piperidinyl 2NCH$_2$), 3.45 (t, 1H, upfield H of pyrrolidinyl *CH*$_2$CH, J = 8.40 Hz), 3.93 (t, 1H, downfield H of pyrrolidinyl *CH*$_2$CH, J = 9.75 Hz), 4.28 (d, 1H, upfield H of NC*H*$_2$N, J = 13.20 Hz), 4.50 (d, 1H, downfield H of NC*H*$_2$N, J = 12.60 Hz), 4.83 (dd, 1H, pyrrolidinyl *CH*CH$_2$, J = 7.80, 10.50 Hz), 6.86–7.41 (m, 13H, 12 arom. H + olefinic CH). Anal. Calcd. for $C_{38}H_{43}N_3O_2$ (573.79): C, 79.55; H, 7.55; N, 7.32. Found: C, 79.63; H, 7.58; N, 7.39.

4.1.10. 1′-Methyl-4′-(4-methylphenyl)-3-[(4-methylphenyl)methylidene]-1″-[(4-morpholinyl)methylene]-dispiro[cyclohexane-1,3′-pyrrolidine-2′,3″-[3H]indole]-2,2″(1″H)-dione (**4j**)

Obtained from **1e**, **2b** and **3**. Reaction time 22 h, colorless crystals from ethanol, mp 215–217 °C, yield (2.03 g) 71%. IR: ν_{max}/cm^{-1} 1713, 1674 (C=O), 1609, 1512. ^{1}H NMR (CDCl$_3$): δ 1.09–1.34 (m, 4H, cyclohexyl H), 2.07 (s, 3H, pyrrolidinyl NCH$_3$), 2.14–2.29 (m, 2H, cyclohexyl H), 2.32 (s, 3H, ArCH$_3$), 2.34 (s, 3H, ArCH$_3$), 2.61 (t, 4H, morpholinyl 2NCH$_2$, J = 4.65 Hz), 3.45 (dd, 1H, upfield H of pyrrolidinyl *CH*$_2$CH, J = 7.80, 8.70 Hz), 3.65 (t, 4H, morpholinyl 2OCH$_2$, J = 4.35 Hz), 3.91 (dd, 1H, downfield H of pyrrolidinyl *CH*$_2$CH, J = 9.30, 10.20 Hz), 4.32 (d, 1H, upfield H of NC*H*$_2$N, J = 12.60 Hz), 4.48 (d, 1H, downfield H of NC*H*$_2$N, J = 12.60 Hz), 4.83 (dd, 1H, pyrrolidinyl *CH*CH$_2$, J = 7.80, 10.20 Hz), 6.84–7.40 (m, 13H, 12 arom. H + olefinic CH). MS: m/z (%) 475 [(M − $C_5H_{10}NO$), 29]. Anal. Calcd. for $C_{37}H_{41}N_3O_3$ (575.76): C, 77.19; H, 7.18; N, 7.30. Found: C, 77.16; H, 7.22; N, 7.41.

4.1.11. 1′-Methyl-4′-(4-methylphenyl)-3-[(4-methylphenyl)methylidene]-1″-[1-(4-methylpiperazinyl)methylene]-dispiro[cyclohexane-1,3′-pyrrolidine-2′,3″-[3H]indole]-2,2″(1″H)-dione (**4k**)

Obtained from **1e**, **2c** and **3**. Reaction time 25 h, pale yellow crystals from ethanol, mp 154–156 °C, yield (1.80 g) 61%. IR: ν_{max}/cm^{-1} 1697, 1667 (C=O), 1593, 1508. ^{1}H NMR (CDCl$_3$): δ 1.07–1.32 (m, 4H, cyclohexyl H), 2.08 (s, 3H, pyrrolidinyl NCH$_3$), 2.13 (s, 3H, piperazinyl NCH$_3$), 2.16–2.30 (m, 2H, cyclohexyl H) 2.32 (s, 3H, ArCH$_3$), 2.34 (s, 3H, ArCH$_3$), 2.39 (br s, 4H, piperazinyl 2NCH$_2$), 2.66 (br s, 4H, piperazinyl 2NCH$_2$), 3.44 (t, 1H, upfield H of pyrrolidinyl *CH*$_2$CH, J = 7.20 Hz), 3.91 (t, 1H, downfield H of pyrrolidinyl *CH*$_2$CH, J = 11.40 Hz), 4.34 (d, 1H, upfield H of NC*H*$_2$N, J = 12.60 Hz), 4.46 (d,

1H, downfield H of NCH_2N, J = 12.90 Hz), 4.83 (dd, 1H, pyrrolidinyl CHCH$_2$, J = 7.80, 10.50 Hz), 6.72–7.40 (m, 13H, 12 arom. H + olefinic CH). ^{13}C NMR ($CDCl_3$): δ 19.7 (cyclohexyl *C*-6), 21.3 (ArCH_3), 21.5 (ArCH_3), 28.9 (cyclohexyl *C*-5), 31.2 (cyclohexyl *C*-4), 35.0 (pyrrolidinyl NCH_3), 46.2 (piperazinyl NCH_3), 49.3 (HC-4′), 51.2 (piperazinyl NH_2C-2/6), 55.0 (piperazinyl NH_2C-3/5), 58.1 (H_2C-5′), 62.2 (NCH_2N), 64.0 [spiro *C*-1 (*C*-3′)], 77.7 [spiro *C*-2′ (*C*-3″)], 109.4, 122.8, 122.9, 128.3, 128.7, 129.08, 129.1, 129.4, 130.2, 130.24, 130.5, 130.6, 133.4, 136.5, 136.8, 137.0, 138.6, 138.8, 141.7, 144.4 (arom. *C* + olefinic *C*), 176.3 [oxindolyl *C*=O (*C*-2″)], 202.9 [cyclohexyl *C*=O (*C*-2)]. Anal. Calcd. for $C_{38}H_{44}N_4O_2$ (588.80): C, 77.52; H, 7.53; N, 9.52. Found: C, 77.68; H, 7.58; N, 9.63.

4.1.12. 4′-(4-Methoxyphenyl)-3-[(4-methoxyphenyl)methylidene]-1′-methyl-1″-[(1-piperidinyl)methylene]-dispiro[cyclohexane-1,3′-pyrrolidine-2′,3″-[3H]indole]-2,2″(1″H)-dione (**4l**)

Obtained from **1f**, **2a** and **3**. Reaction time 20 h, almost colorless crystals from ethanol, mp 170–171 °C, yield (1.80 g) 60%. IR: ν_{max}/cm^{-1} 1701, 1674 (C=O), 1605, 1512. ^{1}H NMR ($CDCl_3$): δ 1.13–1.53 (m, 10H, cyclohexyl 4H + piperidinyl 3CH_2), 2.06 (s, 3H, pyrrolidinyl NCH_3), 2.13–2.41 (m, 2H, cyclohexyl H), 2.56 (t, 4H, piperidinyl 2NCH_2, J = 4.80 Hz), 3.46 (t, 1H, upfield H of pyrrolidinyl CH_2CH, J = 8.55 Hz), 3.79 (s, 3H, OCH_3), 3.80 (s, 3H, OCH_3), 3.89 (t, 1H, downfield H of pyrrolidinyl CH_2CH, J = 9.60 Hz), 4.28 (d, 1H, upfield H of NCH_2N, J = 12.90 Hz), 4.49 (d, 1H, downfield H of NCH_2N, J = 12.60 Hz), 4.78 (dd, 1H, pyrrolidinyl CHCH$_2$, J = 7.95, 10.35 Hz), 6.80–7.45 (m, 13H, 12 arom. H + olefinic CH). ^{13}C NMR ($CDCl_3$): δ 19.8 (cyclohexyl *C*-6), 24.3 (piperidinyl H_2C-4), 26.0 (piperidinyl H_2C-3/5), 29.0 (cyclohexyl *C*-5), 31.4 (cyclohexyl *C*-4), 35.1 (pyrrolidinyl NCH_3), 49.2 (HC-4′), 52.5 (piperidinyl NCH_2-2/6), 55.4 (OCH_3), 55.5 (OCH_3), 58.6 (H_2C-5′), 63.0 (NCH_2N), 63.7 [spiro *C*-1 (*C*-3′)], 77.7 [spiro *C*-2′ (*C*-3″)], 109.5, 113.8, 113.9, 122.7, 126.1, 128.2, 128.9, 129.4, 131.76, 131.8, 132.0, 135.6, 138.8, 144.8, 158.7, 160.0 (arom. *C* + olefinic *C*), 176.5 [oxindolyl *C*=O (*C*-2″)], 202.8 [cyclohexyl *C*=O (*C*-2)]. MS: *m*/*z* (%) 507 [(M − C_6H_{12}N), 14]. Anal. Calcd. for $C_{38}H_{43}N_3O_4$ (605.78): C, 75.34; H, 7.15; N, 6.94. Found: C, 75.35; H, 7.19; N, 7.09.

4.1.13. 4′-(4-Methoxyphenyl)-3-[(4-methoxyphenyl)methylidene]-1′-methyl-1″-[(4-morpholinyl)methylene]-dispiro[cyclohexane-1,3′-pyrrolidine-2′,3″-[3H]indole]-2,2″(1″H)-dione (**4m**)

Obtained from **1f**, **2b** and **3**. Reaction time 22 h, colorless crystals from ethanol, mp 164–166 °C, yield (1.90 g) 63%. IR: ν_{max}/cm^{-1} 1710, 1678 (C=O), 1597, 1512. ^{1}H NMR ($CDCl_3$): δ 1.11–1.33 (m, 4H, cyclohexyl H), 2.07 (s, 3H, pyrrolidinyl NCH_3), 2.13–2.36 (m, 2H, cyclohexyl H), 2.61 (t, 4H, morpholinyl 2NCH_2, J = 4.65 Hz), 3.46 (t, 1H, upfield H of pyrrolidinyl CH_2CH, J = 8.40 Hz), 3.66 (t, 4H, morpholinyl 2OCH_2, J = 4.35 Hz), 3.79 (s, 3H, OCH_3), 3.80 (s, 3H, OCH_3), 3.87 (t, 1H, downfield H of pyrrolidinyl CH_2CH, J = 9.75 Hz), 4.32 (d, 1H, upfield H of NCH_2N, J = 12.60 Hz), 4.48 (d, 1H, downfield H of NCH_2N, J = 12.60 Hz), 4.79 (dd, 1H, pyrrolidinyl CHCH$_2$, J = 7.80, 10.20 Hz), 6.81–7.43 (m, 13H, 12 arom. H + olefinic CH). Anal. Calcd. for $C_{37}H_{41}N_3O_5$ (607.76): C, 73.12; H, 6.80; N, 6.91. Found: 73.14; H, 6.87; N, 7.04.

4.1.14. 4′-(4-Methoxyphenyl)-3-[(4-methoxyphenyl)methylidene]-1′-methyl-1″-[1-(4-methylpiperazinyl)methylene]-dispiro[cyclohexane-1,3′-pyrrolidine-2′,3″-[3H]indole]-2,2″(1″H)-dione (**4n**)

Obtained from **1f**, **2c** and **3**. Reaction time 24 h, pale yellow crystals from ethanol (80%), mp 115–116 °C, yield (2.10 g) 68%. IR: ν_{max}/cm^{-1} 1709, 1670 (C=O), 1605, 1512. ^{1}H NMR ($CDCl_3$): δ 1.15–1.33 (m, 4H, cyclohexyl H), 2.07 (s, 3H, pyrrolidinyl NCH_3), 2.13–2.30 (m, 5H, 2 cyclohexyl H + piperazinyl NCH_3), 2.40 (br s, 4H, piperazinyl 2NCH_2), 2.66 (br s, 4H, piperazinyl 2NCH_2), 3.45 (t, 1H, upfield H of pyrrolidinyl CH_2CH, J = 8.40 Hz), 3.79–3.91 (m, 7H, 2OCH_3 + downfield H of pyrrolidinyl CH_2CH), 4.34 (d, 1H, upfield H of NCH_2N, J = 12.90 Hz), 4.46 (d, 1H, downfield H of NCH_2N, J = 12.90 Hz), 4.79 (dd, 1H, pyrrolidinyl CHCH$_2$, J = 8.25, 10.35 Hz), 6.81–7.43 (m, 13H, 12 arom. H + olefinic CH). Anal. Calcd. for $C_{38}H_{44}N_4O_4$ (620.80): C, 73.52; H, 7.14; N, 9.02. Found: 73.54; H, 7.12; N, 9.18.

4.1.15. 4′-(3,4-Dimethoxyphenyl)-3-[(3,4-dimethoxyphenyl)methylidene]-1′-methyl-1″-[(1-piperidinyl)methylene]-dispiro[cyclohexane-1,3′-pyrrolidine-2′,3″-[3H]indole]-2,2″(1″H)-dione (**4o**)

Obtained from **1g**, **2a** and **3**. Reaction time 22 h, yellow crystals from ethanol (80%), mp 119–120 °C, yield (2.55 g) 77%. IR: ν_{max}/cm^{-1} 1705, 1670 (C=O), 1609, 1589. ^{1}H NMR ($CDCl_3$): δ 1.18–1.65 (m, 10H, cyclohexyl 4H + piperidinyl 3CH_2), 2.07 (s, 3H, pyrrolidinyl NCH_3), 2.18–2.40 (m, 2H, cyclohexyl H), 2.60 (br s, 4H, piperidinyl 2NCH_2), 3.49 (t, 1H, upfield H of pyrrolidinyl CH_2CH, J = 8.55 Hz), 3.84–3.93 (m, 13H, 4OCH_3 + downfield H of pyrrolidinyl CH_2CH), 4.29 (d, 1H, upfield H of NCH_2N, J = 12.90 Hz), 4.56 (d, 1H, downfield H of NCH_2N, J = 12.60 Hz), 4.75 (dd, 1H, pyrrolidinyl CHCH$_2$, J = 7.95, 10.05 Hz), 6.69–7.27 (m, 11H, 10 arom. H + olefinic CH). Anal. Calcd. for $C_{40}H_{47}N_3O_6$ (665.84): C, 72.16; H, 7.12; N, 6.31. Found: C, 72.20; H, 7.11; N, 6.41.

4.1.16. 4′-(3,4-Dimethoxyphenyl)-3-[(3,4-dimethoxyphenyl)methylidene]-1′-methyl-1″-[(4-morpholinyl)methylene]-dispiro[cyclohexane-1,3′-pyrrolidine-2′,3″-[3H]indole]-2,2″(1″H)-dione (**4p**)

Obtained from **1g**, **2b** and **3**. Reaction time 22 h, yellow crystals from ethanol (80%), mp 127–128 °C, yield (2.54 g) 76%. IR: ν_{max}/cm^{-1} 1707, 1670 (C=O), 1609, 1597. ^{1}H NMR ($CDCl_3$): δ 1.20–1.36 (m, 4H, cyclohexyl H), 2.09 (s, 3H, pyrrolidinyl NCH_3), 2.16–2.39 (m, 2H, cyclohexyl H), 2.62 (t, 4H, morpholinyl 2NCH_2, J = 4.65 Hz), 3.50 (t, 1H, upfield H of pyrrolidinyl CH_2CH, J = 8.40 Hz), 3.66 (t, 4H, morpholinyl 2OCH_2, J = 4.35 Hz), 3.84–3.92 (m, 13H, 4OCH_3 + downfield H of pyrrolidinyl CH_2CH), 4.32 (d, 1H, upfield H of NCH_2N, J = 12.60 Hz), 4.51 (d, 1H, downfield H of NCH_2N, J = 12.90 Hz), 4.75 (t, 1H, pyrrolidinyl CHCH$_2$, J = 9.00 Hz), 6.69–7.22 (m, 11H, 10 arom. H + olefinic CH). Anal. Calcd. for $C_{39}H_{45}N_3O_7$ (667.81): C, 70.14; H, 6.79; N, 6.29. Found: 70.21; H, 6.81; N, 6.38.

4.1.17. 4′-(3,4-Dimethoxyphenyl)-3-[(3,4-dimethoxyphenyl)methylidene]-1′-methyl-1″-[1-(4-methylpiperazinyl)methylene]-dispiro[cyclohexane-1,3′-pyrrolidine-2′,3″-[3H]indole]-2,2″(1″H)-dione (**4q**)

Obtained from **1g**, **2c** and **3**. Reaction time 25 h, yellow crystals from ethanol (80%), mp 140–142 °C, yield (1.90 g) 56%. IR: ν_{max}/cm^{-1} 1707, 1670 (C=O), 1607, 1589. ^{1}H NMR ($CDCl_3$): δ 1.12–1.36 (m, 4H, cyclohexyl H), 2.07 (s, 3H, pyrrolidinyl NCH_3), 2.14–2.46 (m, 2H, cyclohexyl H), 2.53 (s, 3H, piperazinyl NCH_3), 2.82 (br s, 4H, piperazinyl 2NCH_2), 2.91 (br s, 4H, piperazinyl 2NCH_2), 3.48 (t, 1H, upfield H of pyrrolidinyl CH_2CH, J = 8.40 Hz), 3.84–3.93 (m, 13H, 4OCH_3, downfield H of pyrrolidinyl CH_2CH), 4.36 (d, 1H, upfield H of NCH_2N, J = 12.90 Hz), 4.54 (d, 1H, downfield H of NCH_2N, J = 12.90 Hz), 4.74 (t, 1H, pyrrolidinyl CHCH$_2$, J = 9.15 Hz), 6.69–7.28 (m, 11H, 10 arom. H + olefinic CH). Anal. Calcd. for $C_{40}H_{48}N_4O_6$ (680.85): C, 70.57; H, 7.11; N, 8.23. Found: 70.64; H, 7.11; N, 8.32.

4.1.18. 1′-Methyl-1″-[(1-piperidinyl)methylene]-4′-(2-thienyl)-3-[(2-thienyl)methylidene]-dispiro[cyclohexane-1,3′-pyrrolidine-2′,3″-[3H]indole]-2,2″(1″H)-dione (**4r**)

Obtained from **1h**, **2a** and **3**. Reaction time 20 h, pale yellow crystals from ethanol, mp 185–187 °C, yield (1.95 g) 70%. IR: ν_{max}/cm^{-1} 1701, 1659 (C=O), 1609, 1562. ^{1}H NMR ($CDCl_3$): δ 1.12–1.60

(m, 10H, cyclohexyl 4H + piperidinyl 3CH_2), 2.06 (s, 3H, pyrrolidinyl NCH_3), 2.13–2.38 (m, 2H, cyclohexyl H), 2.59 (t, 4H, piperidinyl 2NCH_2, J = 4.65 Hz), 3.60 (t, 1H, upfield H of pyrrolidinyl CH_2CH, J = 8.55 Hz), 3.91 (t, 1H, downfield H of pyrrolidinyl CH_2CH, J = 9.45 Hz), 4.32 (d, 1H, upfield H of NCH_2N, J = 12.60 Hz), 4.50 (d, 1H, downfield H of NCH_2N, J = 12.90 Hz), 5.01 (t, 1H, pyrrolidinyl $CHCH_2$, J = 8.85 Hz), 6.89–7.73 (m, 11H, 10 arom. H + olefinic CH). MS: m/z (%) 459 [(M − $C_6H_{12}N$), 21] 461 (2), 463 (0.7). Anal. Calcd. for $C_{32}H_{35}N_3O_2S_2$ (557.78): C, 68.91; H, 6.32; N, 7.53. Found: C, 68.96; H, 6.36; N, 7.57.

4.1.19. 1′-Methyl-1″-[(4-morpholinyl)methylene]-4′-(2-thienyl)-3-[(2-thienyl)methylidene]-dispiro[cyclohexane-1,3′-pyrrolidine-2′,3″-[3H]indole]-2,2″(1″H)-dione (**4s**)

Obtained from **1h**, **2b** and **3**. Reaction time 22 h, pale yellow crystals from ethanol, mp 188–190 °C, yield (2.06 g) 74%. IR: ν_{max}/cm^{-1} 1701, 1667 (C═O), 1605, 1574. ^{1}H NMR ($CDCl_3$): δ 1.41–1.51 (m, 4H, cyclohexyl H), 2.07 (s, 3H, pyrrolidinyl NCH_3), 2.13–2.38 (m, 2H, cyclohexyl H), 2.63 (t, 4H, morpholinyl 2NCH_2, J = 4.65 Hz), 3.60 (t, 1H, upfield H of pyrrolidinyl CH_2CH, J = 8.55 Hz), 3.69 (t, 4H, morpholinyl 2OCH_2, J = 4.65 Hz), 3.90 (t, 1H, downfield H of pyrrolidinyl CH_2CH, J = 9.45 Hz), 4.36 (d, 1H, upfield H of NCH_2N, J = 12.90 Hz), 4.50 (d, 1H, downfield H of NCH_2N, J = 12.90 Hz), 5.01 (dd, 1H, pyrrolidinyl $CHCH_2$, J = 8.10, 9.60 Hz), 6.87–7.70 (m, 11H, 10 arom. H + olefinic CH). Anal. Calcd. for $C_{31}H_{33}N_3O_3S_2$ (559.75): C, 66.52; H, 5.94; N, 7.51. Found: 66.56; H, 5.97; N, 7.58.

4.1.20. 1′-Methyl-1″-[1-(4-methylpiperazinyl)methylene]-4′-(2-thienyl)-3-[(2-thienyl)methylidene]-dispiro[cyclohexane-1,3′-pyrrolidine-2′,3″-[3H]indole]-2,2″(1″H)-dione (**4t**)

Obtained from **1h**, **2c** and **3**. Reaction time 25 h, pale yellow crystals from ethanol (80%), mp 128–130 °C, yield (1.50 g) 52%. IR: ν_{max}/cm^{-1} 1709, 1667 (C═O), 1605, 1566. ^{1}H NMR ($CDCl_3$): δ 1.24–1.53 (m, 4H, cyclohexyl H), 2.06 (s, 3H, pyrrolidinyl NCH_3), 2.13 (s, 3H, piperazinyl NCH_3), 2.15–2.28 (m, 1H, cyclohexyl H), 2.36 (br s, 4H, piperazinyl 2NCH_2), 2.49 (br s, 1H, cyclohexyl H), 2.87 (br s, 4H, piperazinyl 2NCH_2), 3.57 (t, 1H, upfield H of pyrrolidinyl CH_2CH, J = 8.55 Hz), 3.88 (t, 1H, downfield H of pyrrolidinyl CH_2CH, J = 9.60 Hz), 4.40 (d, 1H, upfield H of NCH_2N, J = 12.60 Hz), 4.53 (d, 1H, downfield H of NCH_2N, J = 12.90 Hz), 5.00 (t, 1H, pyrrolidinyl $CHCH_2$, J = 8.85 Hz), 6.72–7.73 (m, 11H, 10 arom. H + olefinic CH). Anal. Calcd. for $C_{32}H_{36}N_4O_2S_2$ (572.80): C, 67.10; H, 6.34; N, 9.78. Found: 67.16; H, 6.31; N, 9.91.

4.1.21. 1′-Methyl-4′-(5-methyl-2-furanyl)-3-[(5-methyl-2-furanyl)methylidene]-1″-[(4-morpholinyl)methylene]-dispiro[cyclohexane-1,3′-pyrrolidine-2′,3″-[3H]indole]-2,2″(1″H)-dione (**4u**)

Obtained from **1i**, **2b** and **3**. Reaction time 22 h, yellow crystals from ethanol, mp 175–177 °C, yield (1.60 g) 58%. IR: ν_{max}/cm^{-1} 1709, 1670 (C═O), 1609, 1566. ^{1}H NMR ($CDCl_3$): δ 1.16–1.51 (m, 4H, cyclohexyl H), 2.02 (s, 3H, pyrrolidinyl NCH_3), 2.08 (br s, 1H, cyclohexyl H), 2.21 (s, 3H, $ArCH_3$), 2.29 (s, 3H, $ArCH_3$), 2.40 (br s, 1H, cyclohexyl H), 2.61 (t, 4H, morpholinyl 2NCH_2, J = 4.35 Hz), 3.49 (t, 1H, upfield H of pyrrolidinyl CH_2CH, J = 8.40 Hz), 3.67 (t, 4H, morpholinyl 2OCH_2, J = 4.35 Hz), 3.78 (t, 1H, downfield H of pyrrolidinyl CH_2CH, J = 9.60 Hz), 4.30 (d, 1H, upfield H of NCH_2N, J = 13.20 Hz), 4.49 (d, 1H, downfield H of NCH_2N, J = 12.60 Hz), 4.62 (t, 1H, pyrrolidinyl $CHCH_2$, J = 9.00 Hz), 5.91–7.35 (m, 9H, 8 arom. H + olefinic CH). ^{13}C NMR ($CDCl_3$): δ 13.8 ($ArCH_3$), 14.1 ($ArCH_3$), 18.6 (cyclohexyl C-6), 28.2 (cyclohexyl C-5), 29.4 (cyclohexyl C-4), 35.0 (pyrrolidinyl NCH_3), 43.8 (HC-4′), 51.5 (morpholinyl NCH_2), 56.7 (H_2C-5′), 62.2 (NCH_2N), 62.3 [spiro C-1 (C-3′)], 67.0 (morpholinyl OCH_2), 77.8 [spiro C-2′ (C-3″)], 106.5, 109.2, 117.8, 122.8, 123.1, 125.5, 125.8, 128.2, 128.5, 129.4, 131.5, 144.6, 150.8, 151.5, 152.8, 155.4 (arom. C + olefinic C), 176.1 [oxindolyl C═O (C-2″)], 200.8 [cyclohexyl C═O (C-2)].MS: m/z (%) 455 [(M − $C_5H_{10}NO$), 41]. Anal. Calcd. for $C_{33}H_{37}N_3O_5$ (555.68): C, 71.33; H, 6.71; N, 7.56. Found: 71.37; H, 6.73; N, 7.64.

4.1.22. 4′-(4-Chlorophenyl)-3-[(4-chlorophenyl)methylidene]-1′-methyl-dispiro[cyclohexane-1,3′-pyrrolidine-2′,3″-[3H]indole]-2,2″(1″H)-dione (**5a**)

Obtained from reaction of **1b**, **2a** and **3**. Reaction time 10 h, colorless crystals from ethanol, mp 198–200 °C (lit. 205–206 °C [52]), yield (1.60 g) 62%.

4.1.23. 4′-(2,4-Dichlorophenyl)-3-[(2,4-dichlorophenyl)methylidene]-1′-methyl-dispiro[cyclohexane-1,3′-pyrrolidine-2′,3″-[3H]indole]-2,2″(1″H)-dione (**5b**)

Obtained from **1c**, **2a**/**2c** and **3**. Reaction time 10, 12 h "for reaction of **1c** with **2a** and **2c**, respectively", colorless crystals from ethanol, mp 241–242 °C, yield (2.28, 2.42 g) 78, 83% "for reaction of **1c** with **2a** and **2c**, respectively". IR: ν_{max}/cm^{-1} 3152 (NH), 1713, 1682 (C═O), 1616, 1589. ^{1}H NMR ($CDCl_3$): δ 1.04–1.39 (m, 4H, cyclohexyl H), 1.96–2.00 (m, 1H, cyclohexyl H), 2.13 (s, 3H, pyrrolidinyl NCH_3), 2.24 (br s, 1H, cyclohexyl H), 3.51 (t, 1H, upfield H of pyrrolidinyl CH_2CH, J = 8.55 Hz), 3.94 (t, 1H, downfield H of pyrrolidinyl CH_2CH, J = 9.30 Hz), 5.11 (t, 1H, pyrrolidinyl $CHCH_2$, J = 9.00 Hz), 6.74–7.98 (m, 12H, 10 arom. H + olefinic CH + NH). Anal. Calcd. for $C_{30}H_{24}Cl_4N_2O_2$ (586.35): C, 61.45; H, 4.13; N, 4.78. Found: C, 61.48; H, 4.13; N, 4.83.

4.2. Single crystal X-ray of compound **4a**

Full crystallographic details of compound **4a**, excluding structure factors have been deposited at Cambridge Crystallographic Data Centre (CCDC) as a supplementary publication number CCDC 948254. Crystals of compound **4a** suitable for single crystal X-ray structure determination were obtained by recrystallization from ethanol using slow evaporation method. The data were collected at T = 298 K on Enraf Nonius 590 Kappa CCD single crystal diffractometer equipped with graphite monochromated MoKα (λ = 0.71073 Å) radiation by using ψ–ω scan technique at room temperature. The crystal to detector distance was 4 cm, cell refinement and data reduction were carried using maXus software [53]. The crystal structures were solved by direct method using SIR92 [54], which revealed the positions of all non-hydrogen atoms and refined by the full matrix least squares refinement based on F^2 using maXus package [53]. The anisotropic displacement parameters of all non-hydrogen atoms were refined, then the hydrogen atoms were introduced as a riding model with C–H = 0.96 Å and refined isotropically. Compound **4a** was recrystallized as prismatic colorless crystals. Chemical formula $C_{36}H_{39}N_3O_2$, M_r = 545.727, monoclinic, crystallizes in space group $C2/c$, Cell lengths "a = 32.0378(6), b = 11.0021(3), c = 20.2411(5) Å", cell angles "α = 90.00, β = 123.327(2), γ = 90.00°", V = 5961.3(2) $Å^3$, Z = 8, D_c = 1.216 mg/m^3, θ values 2.910–27.485°, absorption coefficient μ (Mo-K_α) = 0.08 mm^{-1}, F(000) = 2335. The unique reflections measured 8081 of which 2969 reflections with threshold expression $I > 3\sigma(I)$ were used in the structural analysis. Convergence for 370 variable parameters by least-squares refinement on F^2 with $w = 1/[\sigma^2(F_o^2) + 0.10000\ F_o^2]$. The final agreement factors were R = 0.065 and wR = 0.113 with a goodness-of-fit of 2.618.

4.3. Antitumor activity screening

Antitumor properties of the synthesized compounds were screened in National Cancer Institute, Cairo University, Egypt, using the previously reported standard procedure adopting HEPG2 (liver), HELA (cervical), and PC3 (prostate) [34,35,45]. Cells were

seeded in 96-well microtiter plates at a concentration of 5×10^4–10^5 cell/well in a fresh medium and left for 24 h before treatment with the tested compounds to allow attachment of cells to the wall of the plate. The tested compounds were dissolved in dimethylsulfoxide (DMSO) and diluted 1000-fold in the assay. Different concentrations of the compounds under test (0, 5, 12.5, 25, and 50 μg/ml) were added to the cell monolayer. Triplicate wells were prepared for each individual dose. The monolayer cells were incubated with the tested compounds for 48 h at 37 °C, in atmosphere of 5% CO_2. After 48 h, the cells were fixed, washed and stained with Sulfo-Rhodamine-B (SRB) stain. Excess stain was washed with acetic acid. The attached stain was recovered with Tris–EDTA buffer. Cell survival and drug activity were determined by measuring the color intensity spectrophotometrically at 564 nm using an ELISA microplate reader (Meter tech. Σ 960, USA). Data were collected as mean values for experiments that were performed in three replicates for each individual dose and measured by SRB assay. Control experiments did not exhibit significant changes compared to those using the DMSO vehicle. Doxorubicin was used as a standard reference during the in-vitro bioactivity screening assay. The cell surviving fraction was calculated as follows:

Surviving fraction = Optical density (O.D.) of treated cells/O.D. of control cells.

The IC_{50} (concentration required to produce 50% inhibition of cell growth compared to the control experiment) was determined using Graph-Pad PRISM version-5 software. Statistical calculations for determination of the mean and standard error values were determined by SPSS 11 software. The observed antitumor properties are presented in Table 1 and Figs. 1–3 of the Supplementary material.

Acknowledgment

This work was sponsored by the Swedish International Development Cooperation Agency (SIDA) due to the International Collaborative Research Grant (MENA) to A.S.G. and J.S.

Appendix A. Supplementary data

Supplementary data related to this article can be found at http://dx.doi.org/10.1016/j.ejmech.2013.07.035.

References

[1] M. Nakhjiri, M. Safavi, E. Alipour, S. Emami, A.F. Atash, M. Jafari-Zavareh, S.K. Ardestani, M. Khoshneviszadeh, A. Foroumadi, A. Shafiee, Eur. J. Med. Chem. 50 (2012) 113–123.
[2] Y.L. Chen, S.Z. Lin, J.Y. Chang, Y.L. Cheng, N.M. Tsai, S.P. Chen, W.L. Chang, H.J. Harn, Biochem. Pharmacol. 72 (2006) 308–319.
[3] D. Hanahan, R.A. Weinberg, Cell 100 (2000) 57–70.
[4] C.S.A. Kumar, S.N. Swamy, N.R. Thimmegowda, S.B.B. Prasad, G.W. Yip, K.S. Rangappa, Med. Chem. Res. 16 (2007) 179–187.
[5] S.N. Pandeya, S. Smitha, M. Jyoti, S.K. Sridhar, Acta Pharm. 55 (2005) 27–46.
[6] K.L. Vine, L. Matesic, J.M. Locke, M. Ranson, D. Skropeta, Anti-Cancer Agents Med. Chem. 9 (2009) 397–414.
[7] J. Ma, S. Li, K. Reed, P. Guo, J.M. Gallo, J. Pharmacol. Exp. Ther. 305 (2003) 833–839.
[8] M.E. Lane, B. Yu, A. Rice, K.E. Lipson, C. Liang, L. Sun, C. Tang, G. McMahon, R.G. Pestell, S. Wadler, Cancer Res. 61 (2001) 6170–6177.
[9] A. Millemaggi, R.J.K. Taylor, Eur. J. Org. Chem. (2010) 4527–4547.
[10] J. Liu, H. Sun, X. Liu, L. Ouyang, T. Kang, Y. Xie, X. Wang, Tetrahedron Lett. 53 (2012) 2336–2340.
[11] C.V. Galliford, K.A. Scheidt, Angew. Chem. Int. Ed. 46 (2007) 8748–8758.
[12] C. Marti, E.M. Carreira, Eur. J. Org. Chem. (2003) 2209–2219.
[13] B.M. Trost, M.K. Brennan, Synthesis 18 (2009) 3003–3025.
[14] L. Zhao, B. Zhou, Y. Li, Heteroat. Chem. 22 (2011) 673–677.
[15] M.J. Kornet, A.P. Thio, J. Med. Chem. 19 (1976) 892–898.
[16] A. Jossang, P. Jossang, H.A. Hadi, T. Sévenet, B. Bodo, J. Org. Chem. 56 (1991) 6527–6530.
[17] S. Ghosal, P.K. Banerjee, Indian J. Chem. 9 (1971) 289–293.
[18] K. Jones, J. Wilkinson, J. Chem. Soc. Chem. Commun. (1992) 1767–1769.
[19] S.I. Bascop, J. Sapi, J.Y. Laronze, J. Lévy, Heterocycles 38 (1994) 725–732.
[20] C. Pellegrini, C. Strässler, M. Weber, H.J. Borschberg, Tetrahedron: Asymmetry 5 (1994) 1979–1992.
[21] G. Palmisano, R. Annunziata, G. Papeo, M. Sisti, Tetrahedron: Asymmetry 7 (1996) 1–4.
[22] M.N.G. James, G.J.B. Williams, Can. J. Chem. 50 (1972) 2407–2412.
[23] W.H. Wong, P.B. Lim, C.H. Chuah, Phytochemistry 41 (1996) 313–315.
[24] R.L. Garnick, P.W. Lequesne, J. Am. Chem. Soc. 100 (1978) 4213–4219.
[25] E. Garcia Prado, M.D. Garcia Gimenez, R. De la Puerta Vázquez, J.L. Espartero Sánchez, M.T. Sáenz Rodriguez, Phytomedicine 14 (2007) 280–284.
[26] C.B. Cui, H. Kakeya, H. Osada, Tetrahedron 52 (1996) 12651–12666.
[27] C.B. Cui, H. Kakeya, H. Osada, J. Antibiot. 49 (1996) 832–835.
[28] W. Tang, G. Eisenbrand, Chinese Drugs of Plant Origin, Chemistry, Pharmacology and Use in Traditional and Modern Medicine, Springer-Verlag, Berlin, 1992, pp. 997–1002.
[29] T.H. Kang, Y. Murakami, K. Matsumoto, H. Takayama, M. Kitajima, N. Aimi, H. Watanabe, Eur. J. Pharmacol. 455 (2002) 27–34.
[30] K. Ding, Y. Lu, N.Z. Coleska, S. Qiu, Y. Ding, W. Gao, J. Stuckey, K. Krajewski, P.P. Roller, Y. Tomita, D.A. Parrish, J.R. Deschamps, S. Wang, J. Am. Chem. Soc. 127 (2005) 10130–10131.
[31] (a) Z.M. Nofal, A.M. Srour, W.I. El-Eraky, D.O. Saleh, A.S. Girgis, Eur. J. Med. Chem. 63 (2013) 14–21;
(b) A.S. Girgis, S.R. Tala, P.V. Oliferenko, A.A. Oliferenko, A.R. Katritzky, Eur. J. Med. Chem. 50 (2012) 1–8;
(c) A.S. Girgis, H. Farag, N.S.M. Ismail, R.F. George, Eur. J. Med. Chem. 46 (2011) 4964–4969;
(d) A.S. Girgis, N.S.M. Ismail, H. Farag, Eur. J. Med. Chem. 46 (2011) 2397–2407;
(e) A.R. Katritzky, A.S. Girgis, S. Slavov, S.R. Tala, I. Stoyanova-Slavova, Eur. J. Med. Chem. 45 (2010) 5183–5199;
(f) A.S. Girgis, N.S.M. Ismail, H. Farag, W.I. El-Eraky, D.O. Saleh, S.R. Tala, A.R. Katritzky, Eur. J. Med. Chem. 45 (2010) 4229–4238;
(g) A.S. Girgis, F.F. Barsoum, A. Samir, Eur. J. Med. Chem. 44 (2009) 2447–2451;
(h) F.F. Barsoum, A.S. Girgis, Eur. J. Med. Chem. 44 (2009) 2172–2177;
(i) A.S. Girgis, F.F. Barsoum, Eur. J. Med. Chem. 44 (2009) 1972–1977;
(j) A.S. Girgis, Eur. J. Med. Chem. 43 (2008) 2116–2121;
(k) A.S. Girgis, N. Mishriky, A.M. Farag, W.I. El-Eraky, H. Farag, Eur. J. Med. Chem. 43 (2008) 1818–1827;
(l) A.S. Girgis, N. Mishriky, M. Ellithey, H.M. Hosni, H. Farag, Bioorg. Med. Chem. 15 (2007) 2403–2413;
(m) A.S. Girgis, M. Ellithey, Bioorg. Med. Chem. 14 (2006) 8527–8532;
(n) A.S. Girgis, A. Kalmouch, M. Ellithey, Bioorg. Med. Chem. 14 (2006) 8488–8494;
(o) A.S. Girgis, H.M. Hosni, F.F. Barsoum, Bioorg. Med. Chem. 14 (2006) 4466–4476;
(p) F.F. Barsoum, H.M. Hosni, A.S. Girgis, Bioorg. Med. Chem. 14 (2006) 3929–3937;
(q) A.S. Girgis, H.M. Hosni, F.F. Barsoum, A.M.M. Amer, I.S. Ahmed-Farag, Boll. Chim. Farm. 143 (2004) 365–375;
(r) A.S. Girgis, A. Kalmouch, H.M. Hosni, Amino Acids 26 (2004) 139–146.
[32] A.S. Girgis, Eur. J. Med. Chem. 44 (2009) 1257–1264.
[33] A.S. Girgis, Eur. J. Med. Chem. 44 (2009) 91–100.
[34] A.M. Moustafa, A.S. Girgis, S.M. Shalaby, E.R.T. Tiekink, Acta Crystallogr. Sect. E: Struct. Rep. Online E68 (2012) o2197–o2198.
[35] A.S. Girgis, J. Stawinski, N.S.M. Ismail, H. Farag, Eur. J. Med. Chem. 47 (2012) 312–322.
[36] J.D. Yang, L.R. Roberts, Nat. Rev. Gastroenterol. Hepatol. 7 (2010) 448–458.
[37] M. Schwartz, S. Roayaie, M. Konstadoulakis, Nat. Clin. Pract. Oncol. 4 (2007) 424–432.
[38] F. Donato, P. Boffetta, M. Puoti, Int. J. Cancer 75 (1998) 347–354.
[39] (a) http://www.ncbi.nlm.nih.gov/pubmedhealth/PMH0001895/.
(b) http://www.cancer.gov/cancertopics/types/cervical.
[40] T.L. Veveris-Lowe, M.G. Lawrence, R.L. Collard, L. Bui, A.C. Herington, D.L. Nicol, Endocr. Relat. Cancer 12 (2005) 631–643.
[41] W.G. Nelson, A.M. De Marzo, W.B. Isaacs, New Engl. J. Med. 349 (2003) 366–381.
[42] http://www.cancer.gov/cancertopics/treatment/prostate.
[43] F. Zhang, C.K. Arnatt, K.M. Haney, H.C. Fang, J.E. Bajacan, A.C. Richardson, J.L. Ware, Y. Zhang, Eur. J. Med. Chem. 55 (2012) 395–408.
[44] (a) R. Grigg, S. Thianpatanagul, J. Chem. Soc. Chem. Commun. (1984) 180–181;
(b) R. Grigg, M.F. Aly, V. Sridharan, S. Thianpatanagul, J. Chem. Soc. Chem. Commun. (1984) 182–183;
(c) H. Ardil, R. Grigg, V. Sridharan, S. Suerendrakumar, S. Thianpatanagul, S. Kanajan, J. Chem. Soc. Chem. Commun. (1986) 602–604;
(d) A.R. Suresh Babu, R. Raghunathan, G. Gayatri, G. Narahari Sastry, J. Heterocycl. Chem. 43 (2006) 1467–1472.
[45] P. Skehan, R. Storeng, D. Scudiero, A. Monks, J. McMahon, D. Vistica, J.T. Warren, H. Bokesch, S. Kenney, M.R. Boyd, J. Natl. Cancer Inst. 82 (1990) 1107–1112.

[46] S.Z. Vatsadze, M.A. Manaenkova, N.V. Sviridenkova, N.V. Zyk, D.P. Krut'ko, A.V. Churakov, M.Yu. Antipin, J.A.K. Howard, H. Lang, Russ. Chem. Bull. Int. Ed. 55 (2006) 1184–1194.
[47] N. Singh, J. Pandey, A. Yadav, V. Chaturvedi, S. Bhatnagar, A.N. Gaikwad, S.K. Sinha, A. Kumar, P.K. Shukla, R.P. Tripathi, Eur. J. Med. Chem. 44 (2009) 1705–1709.
[48] P.J. Smith, J.R. Dimmock, W.A. Turner, Can. J. Chem. 51 (1973) 1458–1470.
[49] M.S. El-Hossini, A.M. Khalil, A.I. Osman, F.Z. El-Ablac, J. Indian Chem. Soc. 65 (1988) 636–639.
[50] V.R. Solomon, C. Hu, H. Lee, Bioorg. Med. Chem. 17 (2009) 7585–7592.
[51] A.T. Taher, N.A. Khalil, E.M. Ahmed, Arch. Pharm. Res. 34 (2011) 1615–1621.
[52] A.A. Raj, R. Raghunathan, Tetrahedron 57 (2001) 10293–10298.
[53] S. Mackay, C.J. Gilmore, C. Edwards, N. Stewart, K. Shankland, maXus Computer Program for the Solution and Refinement of Crystal Structures. Bruker Nonius, The Netherlands, MacScience, Japan, The University of Glasgow, 1999.
[54] A. Altomare, G. Cascarano, C. Giacovazzo, A. Guagliardi, M.C. Burla, G. Polidori, M. Camalli, J. Appl. Crystallogr. 27 (1994) 435–436.